

# SimMerge: Learning to Select Merge Operators from Similarity Signals

Oliver Bolton<sup>1</sup>, Aakanksha<sup>2</sup>, Arash Ahmadian<sup>3</sup>, Sara Hooker<sup>4</sup>,  
Marzieh Fadaee<sup>1</sup>, and Beyza Ermis<sup>1</sup>

<sup>1</sup>Cohere Labs, <sup>2</sup>Cohere, <sup>3</sup>Google, <sup>4</sup>Adaption Labs

Corresponding authors: [{beyza, marzieh}@cohere.com](mailto:{beyza, marzieh}@cohere.com)

## Abstract

Model merging enables multiple large language models (LLMs) to be combined into a single model while preserving performance. This makes it a valuable tool in LLM development, offering a competitive alternative to multi-task training. However, merging can be difficult at scale, as successful merging requires choosing the right merge operator, selecting the right models, and merging them in the right order. This often leads researchers to run expensive merge-and-evaluate searches to select the best merge. In this work, we provide an alternative by introducing SIMMERGE, a *predictive merge-selection method* that selects the best merge using inexpensive, task-agnostic similarity signals between models. From a small set of unlabeled probes, we compute functional and structural features and use them to predict the performance of a given 2-way merge. Using these predictions, SIMMERGE selects the best merge operator, the subset of models to merge, and the merge order, eliminating the expensive merge-and-evaluate loop. We demonstrate that we surpass standard merge-operator performance on 2-way merges of 7B-parameter LLMs, and that SIMMERGE generalizes to multi-way merges and 111B-parameter LLM merges without retraining. Additionally, we present a bandit variant that supports adding new tasks, models, and operators on the fly. Our results suggest that learning how to merge is a practical route to scalable model composition when checkpoint catalogs are large and evaluation budgets are tight.

## 1 Introduction

Model merging is a practical approach for composing checkpoints trained on complementary subsets or domain-specific objectives, producing a single model that aggregates their capabilities with modest additional data or compute. Early approaches such as simple parameter averaging and related weight-space operations improved accuracy and robustness, motivating a broad line of methods for composing models in parameter space [Wortsman et al., 2022; Ilharco et al., 2023; Matena & Raffel, 2022]. More recent work proposes structured or interference-aware rules that make merging more reliable across tasks and initializations [Yadav et al., 2023; Huang et al., 2024; Stoica et al., 2024], as well as perspectives that explain or facilitate merging through subspace matching and permutation alignment [Tam et al., 2023; Ainsworth et al., 2022]. Tooling further standardizes implementations and recipes, making merging accessible at scale [Goddard et al., 2024].

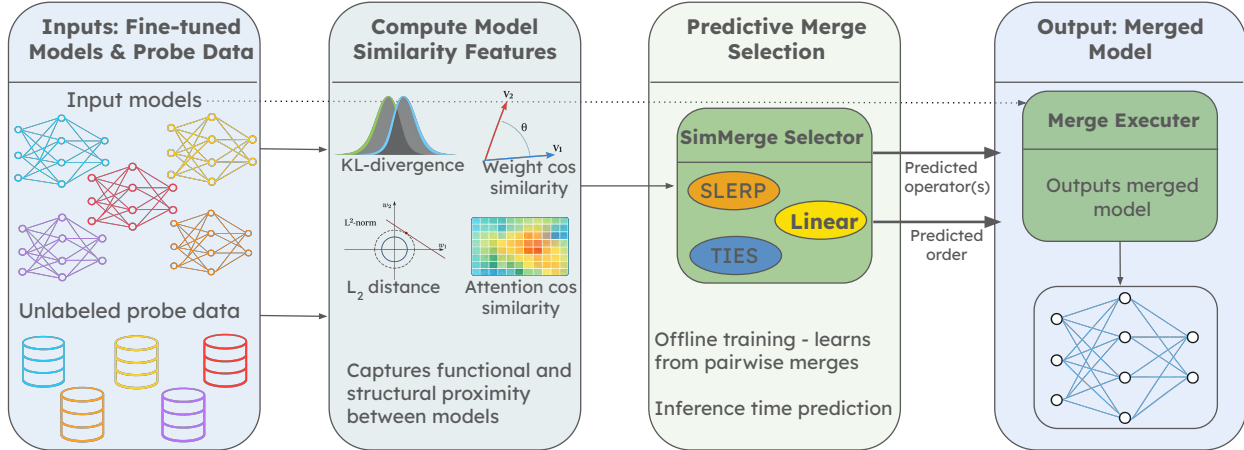


Figure 1: Overview of SIMMERGE. Given a set of domain-specialized checkpoints and small unlabeled probe set for each domain, we compute pre-merge similarity signals, predict the merge operator for each binary merge step and the merge order, and then execute the selected plan once to obtain a single merged model.

As modern LLM development produces thousands of fine-tuned checkpoints across tasks, modalities, and languages, model composition is becoming a central requirement for scalable AI systems. In this work, we study merging post-trained checkpoints: fine-tuned LLMs derived from a shared pretrained base.

At this scale, the bottleneck shifts from **how to merge** to **how to choose a merge configuration**. Given a large catalog, practitioners must decide which models to combine, which operator to apply, and, for multiway merging, in what order. The standard workflow relies on empirical search, where each candidate configuration requires a merge followed by downstream evaluation. Even with efficient operator implementations or data-free heuristics, the cost grows quickly with the number of candidate models, operators, and merge orders, making exhaustive search impractical. Beyond cost, the choice is also sensitive: the same fixed operator can be strong in one domain and harmful in another, so a single global recipe is unreliable in practice.

We address this bottleneck with **predictive merge selection**. We introduce **SIMMERGE**, a lightweight *trained selector* that predicts the merge operator and, for multiway merges, the merge order using inexpensive, task-agnostic similarity measurements between source checkpoints before merging. Unlike prior work that proposes merge operators or tunes merging hyperparameters [Matena & Raffel, 2022; Yadav et al., 2023; Tam et al., 2023; Ainsworth et al., 2022; Stoica et al., 2024; Huang et al., 2024; Akiba et al., 2024], SIMMERGE learns the selection decision from pre-merge similarity signals. Using a small set of unlabeled probes, we compute functional and structural features such as KL divergence between model logits, cosine similarity of weights and attention patterns, and  $\ell_2$  distance in parameter space. These signals are far cheaper than running many merge-and-evaluate trials yet are informative about which configuration will succeed for a given set of models.

SIMMERGE is not a new merge operator; it learns when to apply existing ones. In the pairwise setting, it selects among linear interpolation [Wortsman et al., 2022], spherical linear interpolation (SLERP) [Shoemake, 1985], and TIES merging [Yadav et al., 2023]. New operators can be added as candidates without changing the framework. The selector is trained offline on previously observed merges: for each candidate pair and operator, we record downstream performance and learn to predict the configuration that maximizes it. At deployment time, SIMMERGE requires only the checkpoints and a small unlabeled probe set. It performs no downstream evaluation and applies no gradient-based fine-tuning.

Predictive selection is especially valuable for multiway merging, where operator choice alone is insufficient. Common merge operators are not associative, so different merge orders can produce different models. The number of possible orders grows rapidly with the number of models, making merge-and-evaluate search infeasible at scale. SIMMERGE instead selects a merge plan directly from pre-merge similarity signals. Although trained only on pairwise merges, the similarity-based decision rule extends to multiway settings by scoring plans from the same features, enabling effective three- and four-way merges without extra supervision.

Finally, we consider deployment settings where the model pool and task distribution evolve over time. Offline selectors can drift when new checkpoints or operators appear. We develop an online variant based on a contextual bandit that updates under partial feedback, preserving the low-cost selection step at inference time. Empirically, SIMMERGE is effective on two- to four-way merges of 7B models across multilingual, code, math, and RAG, and transfers to a 111B model without retraining, reducing expert degradation at scale.

Our key contributions are:

- We introduce SIMMERGE, a *predictive merge selection* method that chooses the model subset, merge operator, and merge order using inexpensive similarity metrics between checkpoints, eliminating costly merge-and-evaluate search.
- We extend pairwise operator selection to multiway merging by scoring entire merge plans using the same pairwise similarity features, representing each plan as an ordered sequence of pairwise merges. We also show this approach scales from 7B to 111B-parameter models without retraining.
- We introduce an online contextual bandit variant of SIMMERGE that adapts under partial feedback and supports adding new tasks, models, and operators on-the-fly, allowing for continual deployment in evolving checkpoint catalogs.
- We conduct extensive empirical evaluations across 2-, 3-, and 4-way merges on code, math, multilingual, RAG, and instruction tasks, demonstrating that SIMMERGE consistently outperforms the best fixed merge operator. Averaged over the tasks, SIMMERGE closes 65.0% of the expert-off-domain performance gap, compared to 41.8% for the best single fixed operator.

## 2 Methodology

We consider a catalog of domain-specialized language model checkpoints that we would like to combine into a single model that performs well across a set of target tasks. Let  $\mathcal{T}$  denote the set of evaluation tasks spanning these domains. The goal is to construct a composite model  $\tilde{m}$  that achieves high performance on all tasks in  $\mathcal{T}$ .

Let  $\theta(m) \in \mathbb{R}^d$  denote the parameters of model  $m$ . We work with layerwise binary merge operators  $M_o$  indexed by  $o \in \mathcal{O}$ . Given two models  $m_a, m_b$  and a mixing coefficient  $\alpha \in [0, 1]$ , an operator produces merged parameters

$$\tilde{\theta} = M_o(\theta(m_a), \theta(m_b); \alpha) \in \mathbb{R}^d.$$

In all main experiments we use equal-weight merges with  $\alpha = 0.5$  and take  $\mathcal{O} = \{\text{LINEAR}, \text{SLERP}, \text{TIES}\}$ , where LINEAR is standard linear interpolation, SLERP is spherical linear interpolation, and TIES (trim, elect sign and merge) is a sign-consistent merge. Formal definitions of operators are detailed in Appendix A.

Given models  $\{m_{i_1}, \dots, m_{i_k}\}$ , a  $k$ -way merge plan is an ordered sequence,

$$\pi = (m_{i_1} \rightarrow m_{i_2} \rightarrow \dots \rightarrow m_{i_k}),$$

realized as  $k - 1$  sequential applications of binary merge operators. Concretely, for an operator sequence  $\mathbf{o} = (o_1, \dots, o_{k-1})$  with  $o_t \in \mathcal{O}$ , the plan is executed by repeatedly merging the current model with the next model in  $\pi$  using  $M_{o_t}$ . Because merge operators are not associative, both the order  $\pi$  and the per-step operator choices  $\mathbf{o}$  affect the final merged model and its utility on tasks in  $\mathcal{T}$ . As a result, naive scheme that enumerates all orders and operator choices is quickly intractable: there are  $k!$  possible orders and  $|\mathcal{O}|^{k-1}$  operator sequences, for a total of  $k! |\mathcal{O}|^{k-1}$  candidate configurations.

SIMMERGE is designed to avoid this cost. It precomputes similarity features for each ordered pair of models and task, learns an operator selector from labeled 2-way merges, and then scores and executes multiway merge plans using only these pre-merge signals. Figure 1 gives an end-to-end view of SIMMERGE. Given a set of checkpoints and small unlabeled probe sets, SIMMERGE predicts which operator to use at each binary merge step and which merge order to follow (for  $k > 2$ ). When we require a single merged model for a task set  $\mathcal{T}$ , we score candidate configurations by aggregating predicted utility across tasks, using macro-averaging over  $t \in \mathcal{T}$ .

## 2.1 Setup and Similarity Features

For every ordered pair of models  $(m_a, m_b)$  and task  $t \in \mathcal{T}$ , SIMMERGE computes a similarity feature vector

$$x(m_a, m_b, t) \in \mathbb{R}^m$$

from an unlabeled probe set and the model weights. These signals are inexpensive to obtain and capture both functional behavior and structural alignment. For each task  $t$  we draw an unlabeled probe set  $\mathcal{P}_t$  from the input distribution of  $t$  and compute all data-based metrics on  $\mathcal{P}_t$ . Probe sizes are reported in Section 3.5.

Given an ordered pair  $(m_a, m_b)$ , we first compute measures of functional proximity on  $\mathcal{P}_t$ , including the Kullback-Leibler divergence  $D_{\text{KL}}(p_a \parallel p_b)$  between predictive distributions, optionally computed per layer and then aggregated, and cosine similarities between intermediate activations  $h_a^{(\ell)}$  and  $h_b^{(\ell)}$  at each layer  $\ell$ , averaged over inputs and layers. We then compute weight-based measures that compare models directly in parameter space, including cosine similarity between flattened parameter vectors  $\theta(m_a)$  and  $\theta(m_b)$ , Euclidean distance  $\|\theta(m_a) - \theta(m_b)\|_2$ , and the individual norms  $\|\theta(m_a)\|_2$  and  $\|\theta(m_b)\|_2$ . We additionally include cosine similarity of attention patterns as a separate feature channel.

Each metric yields either a scalar or a short sequence over layers or modules. To obtain a fixed-dimensional representation, sequence-valued metrics are summarized using robust statistics such as the mean, median, and selected quantiles, and all summaries are concatenated into  $x(m_a, m_b, t)$ . By default, we append a task encoding  $c(t) \in \mathbb{R}^{d_c}$  and use

$$\tilde{x}(m_a, m_b, t) = x(m_a, m_b, t) \oplus c(t) \in \mathbb{R}^{m+d_c}$$

as the input to all learned components. We also evaluate a task-agnostic variant that omits  $c(t)$  and report the comparison in Appendix F.1. The improvement from task encoding is modest but consistent, so we use it by default. Full details of the similarity metrics and aggregations are given in Appendix B.

**Computation cost.** Probe-based features scale linearly with the number of probe tokens and require only forward passes. In our experiments, we use only 10000 probe tokens per task, and we cache per-checkpoint outputs so pairwise comparisons reduce to inexpensive post-processing. Weight-based features require a single pass over the parameters (linear in model size), and the overall cost is far lower than running merge-and-evaluate searches.

## 2.2 Predictive Merge Selection

SIMMERGE replaces merge-and-evaluate search with a prediction policy that uses only pre-merge similarity signals. For a target task  $t$ , the policy selects a merge operator for each binary merge step. When  $k > 2$ , it also selects the merge order in which those steps are applied.

**Pairwise operator selection.** For each ordered pair  $(m_a, m_b)$  of models, each task  $t \in \mathcal{T}$ , and each operator  $o \in \mathcal{O}$ , we construct a 2-way merge example as follows. We compute the feature vector  $\tilde{x}(m_a, m_b, t)$ , merge the models with  $M_o$  at  $\alpha = 0.5$  to obtain  $\tilde{m}_o$ , and evaluate  $\tilde{m}_o$  on a held-out validation set for task  $t$ , yielding a utility score

$$s(o; m_a, m_b, t) := \text{score}(\tilde{m}_o, t).$$

The pairwise label is defined as

$$y^*(m_a, m_b, t) = \arg \max_{o \in \mathcal{O}} s(o; m_a, m_b, t).$$

We also record the per-operator utilities  $(s(o; m_a, m_b, t))_{o \in \mathcal{O}}$ .

The pairwise operator selector is a function  $f_{\text{op}} : \mathbb{R}^{m+d_c} \rightarrow \mathcal{O}$  that takes  $\tilde{x}(m_a, m_b, t)$  as input and predicts the merge operator that maximizes downstream utility for the pair  $(m_a, m_b)$  on task  $t$ . In our offline experiments  $f_{\text{op}}$  is instantiated as a lightweight multi-class predictor that outputs a categorical distribution over  $\mathcal{O}$  and is trained with a cross-entropy loss to predict  $y^*$ . Architectural details are given in Section 3.5.

At inference time, given a new pair  $(m_a, m_b)$  and a task  $t$ , SIMMERGE computes  $\tilde{x}(m_a, m_b, t)$ , applies  $f_{\text{op}}$  to obtain scores over operators, selects  $\hat{o} \in \mathcal{O}$  by taking  $\arg \max$ , and returns the merged model  $\tilde{m}_{\hat{o}} = M_{\hat{o}}(m_a, m_b; 0.5)$ . This replaces an exhaustive loop over all operators with a single guided merge.

**Multi-way plan representation and scoring.** To handle  $k$ -way merges, SIMMERGE scores candidate merge plans using only pairwise similarity features. Given a plan  $\pi = (m_{i_1} \rightarrow m_{i_2} \rightarrow \dots \rightarrow m_{i_k})$  and a task  $t$ , we build an order-aware representation by concatenating feature blocks for each step,

$$X(\pi, t) = [x(m_{i_1}, m_{i_2}, t), x(m_{i_2}, m_{i_3}, t), \dots, x(m_{i_{k-1}}, m_{i_k}, t)] \oplus c(t) \in \mathbb{R}^D.$$

This encoding preserves both directionality and step position; different orders induce different  $X(\pi, t)$ . For steps that involve an intermediate merged model, we approximate the required similarity features by propagating metrics from the original pairwise table as described in Appendix D. All blocks are produced by the same similarity encoder used in the pairwise setting.

A plan scorer  $f_{\text{plan}} : \mathbb{R}^D \rightarrow \mathbb{R}$  then assigns a scalar score to each candidate plan. In practice  $f_{\text{plan}}$  is an MLP that shares the similarity encoder with  $f_{\text{op}}$  but has its own final layers. Training  $f_{\text{plan}}$  does not require manual annotations. We obtain targets by executing sampled  $k$ -way plans and

evaluating the resulting merged model on task  $t$ , yielding a utility  $U(\pi, t)$ , and train  $f_{\text{plan}}(X(\pi, t))$  to regress toward  $U(\pi, t)$  over a collection of plans and tasks. A theoretical justification for why pairwise-derived supervision can extend to multiway planning is given in Appendix C.

In the multilingual-code-math-RAG setting, for example, this procedure can yield a plan that first merges  $m_{\text{code}}$  and  $m_{\text{math}}$  using TIES, then adds  $m_{\text{multi}}$  using SLERP, and finally incorporates  $m_{\text{rag}}$  using LINEAR, with all choices inferred from pre-merge similarity features rather than by evaluating every candidate plan.

**Propagating metrics to intermediate merges.** Multi-way plans involve intermediate merged models, such as the result of merging  $m_{i_1}$  and  $m_{i_2}$  before comparing to  $m_{i_3}$ . Recomputing similarity signals for every hypothetical intermediate model would largely negate the computational savings of SIMMERGE. Instead, we approximate similarities involving intermediate merges by propagating metrics from the original pairwise table using convexity properties and standard inequalities. For distributional metrics on probe-set predictions, we treat the intermediate model as an equal-weight mixture of its two parents on the probe set, which yields simple upper bounds for divergences. We fix  $\alpha = 0.5$  in all experiments to isolate the effects of merge operator and merge order, because tuning  $\alpha$  adds a separate hyperparameter search that can confound attribution and reintroduce the expensive search loop.

For predictive distributions  $P_a$ ,  $P_b$ , and  $Q_c$  on the probe set, convexity of  $f$ -divergences yields upper bounds on terms such as

$$\text{KL}((1 - \alpha)P_a + \alpha P_b \parallel Q_c) \quad \text{and} \quad \text{KL}(Q_c \parallel (1 - \alpha)Q_a + \alpha Q_b)$$

in terms of  $\text{KL}(P_a \parallel Q_c)$  and  $\text{KL}(P_b \parallel Q_c)$ . Similarly, if  $\theta_a, \theta_b, \theta_c$  denote flattened parameter vectors, the triangle inequality gives

$$\|(1 - \alpha)\theta_a + \alpha\theta_b - \theta_c\|_2 \leq (1 - \alpha)\|\theta_a - \theta_c\|_2 + \alpha\|\theta_b - \theta_c\|_2.$$

Cosine similarities between mixtures and third models are approximated using convex combinations of pairwise cosines and norms, together with bounds derived from Cauchy-Schwarz. These constructions can be applied layerwise or modulewise and the resulting propagated metrics are aggregated with the same statistics used in Section 2.1 and inserted into  $X(\pi, t)$  whenever a similarity involving an intermediate merge is required. Full formulas and derivations are provided in Appendix D.

At test time, given a subset of models and a task  $t$ , SIMMERGE enumerates or samples a small set of candidate plans, builds  $X(\pi, t)$  for each using the original and propagated metrics, scores them with  $f_{\text{plan}}$ , selects the highest-scoring plan  $\hat{\pi}$ , and executes  $\hat{\pi}$  as a sequence of pairwise merges, choosing the operator at each step via  $f_{\text{op}}$ .

## 2.3 Bandit View and Evaluation Protocol

The offline selector  $f_{\text{op}}$  works well under the distribution of model pairs and tasks seen during training, but it requires to be retrained when new models or tasks are introduced. To support such scenarios without retraining the similarity encoder, we also view operator selection as a contextual bandit problem and add a linear bandit layer on top of the learned features. We then evaluate both the offline and bandit variants in pairwise and multiway regimes.

**Contextual bandit formulation.** Each merge step, either a standalone 2-way merge or a step inside a multiway plan, defines a decision round. We observe a context vector  $s \in \mathbb{R}^m$  derived from

pre-merge similarity features. For pairwise merges, we take  $s = \tilde{x}(m_a, m_b, t)$ . For multiway merges,  $s$  is constructed analogously but may include propagated similarity features for intermediate merges. We then choose an action  $a$  from the finite set of operators  $\mathcal{A} = \{\text{LINEAR}, \text{SLERP}, \text{TIES}\}$ , apply the corresponding merge operator, and observe a scalar reward  $r(a)$  given by the downstream evaluation score. Rewards for unchosen operators are not observed. The objective is to learn a policy  $\pi(s)$  mapping contexts to operators that maximizes cumulative reward, or equivalently minimizes regret with respect to an oracle that always picks the best operator for each context.

We adopt a neural-linear design. An MLP feature map  $g_\phi$  transforms the context  $s$  into a representation  $z(s) = g_\phi(s)$ . We initialize  $g_\phi$  and warm-start it using the logged pairwise data described below, then keep it fixed during online adaptation. On top of  $z(s)$  we fit a linear contextual bandit: for each operator  $a \in \mathcal{A}$  we assume a linear reward model

$$\mathbb{E}[r(a) | z(s)] \approx w_a^\top z(s),$$

with an unknown parameter vector  $w_a$  and a Gaussian posterior  $\mathcal{N}(\hat{w}_a, \Sigma_a)$  maintained via Bayesian linear regression. We consider both LinUCB and linear Thompson sampling (LinTS) [Abbasi-Yadkori et al., 2011; Agrawal & Goyal, 2013]. Empirically LinTS produces lower regret and higher downstream performance in our setting, and we therefore use it as the main bandit variant. Since we have a small number of operators and a low-dimensional representation, posterior updates can be done with rank-one updates in  $O(d^2)$  time per round, where  $d$  is the dimension of  $z(s)$ .

**Warm-start and online adaptation.** The bandit is initialized using the fully-observed pairwise merge dataset constructed in the offline setting. For each historical 2-way merge we know the context and the realized utilities  $s_o$  for all operators  $o \in \mathcal{A}$ , which corresponds to full-information feedback. These logs are used once to fit a Bayesian linear model for each arm, yielding initial posteriors  $(\hat{w}_a, \Sigma_a)$ . This warm-start phase anchors the reward model before any online interaction and reduces the amount of exploration required when new tasks or models are introduced.

After warm-start, we introduce a distribution shift by adding a checkpoint trained on a different task that did not appear in the logged data. For each new merge involving this checkpoint, we compute the context  $s$  from pre-merge similarity signals, query the bandit to select an operator  $a$ , execute  $M_a$ , and observe the resulting reward  $r(a)$  from downstream evaluation. Only the posterior of arm  $a$  is then updated. This is the partial-feedback regime where counterfactual rewards for unchosen operators are not observed.

### 3 Experimental Setup

We evaluate SIMMERGE on four domains: code generation, mathematical reasoning, multilingual understanding and RAG. Within each model scale, all checkpoints share the same pretrained base and architecture, so performance differences arise from task-specific fine-tuning and merging rather than capacity mismatches. At the 7B scale, we use Command-A 7B as the shared pretrained base for all domain-specialized checkpoints. At the larger scale, we use Command-A 111B as the shared base for all 111B experiments [Cohere et al., 2025].

Given a target task  $t$  and a set of  $k$  models to merge, we compare three fixed merge operators, *Linear*, *SLERP*, and *TIES*, against our learned selector SIMMERGE. The fixed baselines apply their respective operator at every merge step within a configuration. For  $k > 2$ , they also use a fixed merge order. In contrast, SIMMERGE does not introduce a new merge rule. It selects among *{Linear, SLERP, TIES}* from pre-merge similarity signals (Section 2) and applies the selected operator once per merge step. For  $k > 2$ , SIMMERGE additionally selects a favorable merge order using the same

similarity signals. Any improvement of SIMMERGE over the fixed baselines therefore comes from predicting the operator choice and, in the multiway setting, the merge order, without running a merge-and-evaluate search.

### 3.1 Experts and Auxiliary Models

**Tasks and experts.** For each of the four domains: code, math, multilingual, RAG, we fine-tune a shared base model on task-specific data to obtain a *task expert* checkpoint  $m_t^{\text{exp}}$ . This expert provides a strong reference point for task  $t$ , since it is the best single model we obtain by standard fine-tuning on  $t$ .

**Auxiliary models.** We refer to any model that is *not* fine-tuned on  $t$  as an *auxiliary* (off-domain) model for task  $t$ . Concretely, when evaluating task  $t$ , the experts of the other domains act as auxiliaries. In the simplest case, we merge the task expert  $m_t^{\text{exp}}$  with a single auxiliary  $m_t^{\text{aux}}$ . For instance, when evaluating on the code task, the code expert is  $m_{\text{code}}^{\text{exp}}$  and the math expert is treated as an auxiliary  $m_{\text{code}}^{\text{aux}}$ . In larger- $k$  merges, we combine one expert with multiple auxiliaries  $\{m_{t,j}^{\text{aux}}\}_j$ . We always report the standalone performance of  $m_t^{\text{exp}}$  and of the corresponding auxiliary model(s) for  $t$  as natural upper- and lower-bound baselines.

Across all offline 7B experiments we use 85 unique domain-specialized checkpoints: 23 code, 24 math, 24 multilingual, and 15 RAG models. For the online bandit experiments we introduce an additional 15 *instruct* checkpoints at 7B, for a total of 100 distinct 7B models. At the larger 111B scale, we use additional 18 task-specific checkpoints (5 code, 5 math, 4 multilingual, and 4 RAG), used only for evaluation.

### 3.2 Merge Configurations

**Pairwise merges.** We first study pairwise merges between a task expert and a single auxiliary. These experiments provide training data for our selectors and test whether similarity signals are sufficient to predict which operator works best for a given expert-auxiliary pair.

The pairwise dataset used for offline training comprises 240 distinct expert-auxiliary merges. Among these training merges, the best-performing operator is Linear in 96 cases, SLERP in 88, and TIES in 56, indicating that no single fixed operator dominates. For offline evaluation, we construct a held-out test set of 60 additional expert-auxiliary pairs. For each of these test pair we evaluate all three operators and log the best-performing method. We use this label to assess the selector’s predictive accuracy, with detailed classifier results reported in Appendix F.1. All evaluation splits are disjoint from the pairwise training data at the pair level where no expert-auxiliary pair used to fit the selector appears in the held-out pairwise test set or in any 3-way or 4-way configuration.

**Multi-way merges.** We then consider 3-way and 4-way merges, selecting models so that there is at most one expert for each task within a single merge. We merge one task expert with auxiliaries from different domains and apply the same set of operators: Linear, SLERP, TIES, SIMMERGE. For  $k > 2$  the merge order affects the result, we therefore evaluate both random-order baselines and the order proposed by our multiway selector. In total we construct 145 distinct 3-way merge configurations and 130 distinct 4-way configurations. Each configuration is evaluated with all three fixed operators and with SIMMERGE, yielding a large corpus of merge outcomes on which to assess the quality of multiway planning.

**Scaling to a larger model.** To test transfer across scales, we repeat the 3-way merging experiments

with a substantially larger base model with 111B parameters, using the same similarity features and selector architectures trained on the smaller 7B models. At 111B, we construct an evaluation set of 100 3-way merge configurations to test whether a selector trained at one scale can be reused at a larger scale without retraining.

**Online evaluation merges.** For the linear bandit experiments, we generate a separate test set of merge configurations that includes the additional *instruct* checkpoints. This bandit evaluation set contains 60 merge instances for 2-, 3-, and 4-way merges and is constructed to be disjoint from the pairwise training data at the pair level, meaning no ordered model pair appearing in the bandit evaluation appears in the offline pairwise training set.

### 3.3 Evaluations

We evaluate expert and merged models on held-out evaluation sets covering our four core domains, plus an instruction-following suite used in the bandit experiments.

**Per-task evaluations.** For each task  $t$ , we evaluate on a small collection of standard benchmarks (details in Appendix E). Math is evaluated on MATH [Hendrycks et al., 2021] and GSM8K [Zeng et al., 2023] using exact match. Multilingual performance is measured on an internal multilingual QA suite together with MGSM [Shi et al., 2022], using win-rates and accuracy. Code generation is evaluated with *pass@1* on HumanEval\_Python [Chen, 2021] and MBPP+ benchmark [Liu et al., 2023]. For RAG, we use TauBench [Yao et al., 2025] and BFCL [Patil et al., 2025] with accuracy and F1. In the instruction-following setting used for the bandit experiments, we report scores on IFEval [Zhou et al., 2023]. We run each evaluation three times with different seeds and report the mean score.

**Task-level aggregation.** To obtain a single score per task, we average the metric over all evaluations associated with that task. All aggregation is done separately for each merging method, so that comparisons between experts, auxiliaries, and merges are on the same task-specific scale.

### 3.4 Metrics

We evaluate merge quality using both absolute task performance and normalized improvements over two natural baselines. For a model  $m$  on task  $t$ , define the expert baseline score

$$s_{\text{expert}}(t) := \text{score}(\text{expert}_t, t),$$

and the auxiliary baseline score  $s_{\text{aux}}(t)$  as follows: for pairwise merges,  $s_{\text{aux}}(t) := \text{score}(\text{aux}_t, t)$  where  $\text{aux}_t$  is the single auxiliary model paired with  $\text{expert}_t$  and for multiway merges,

$$s_{\text{aux}}(t) := \frac{1}{|\mathcal{A}_t|} \sum_{m' \in \mathcal{A}_t} \text{score}(m', t),$$

where  $\mathcal{A}_t$  is the set of auxiliary models included in that merge configuration. We then report normalized improvements:

$$\begin{aligned} \Delta_{\text{expert}}(m, t) &= 100 \cdot \frac{\text{score}(m, t) - s_{\text{expert}}(t)}{s_{\text{expert}}(t)}, \\ \Delta_{\text{aux}}(m, t) &= 100 \cdot \frac{\text{score}(m, t) - s_{\text{aux}}(t)}{s_{\text{aux}}(t)}. \end{aligned}$$

We aggregate over tasks by macro-averaging  $\Delta_{\text{expert}}(m, t)$  and  $\Delta_{\text{aux}}(m, t)$  across  $t \in \mathcal{T}$ . These normalized metrics account for scale differences across tasks and benchmarks and enable fair cross-domain comparisons.

In addition, we report absolute performance (macro-averaged score( $m, t$ )) to anchor relative improvements on the original task scales.

In addition to  $\Delta_{\text{expert}}$  and  $\Delta_{\text{aux}}$ , we also report results using the *gap closed* metric, which summarizes how much of the performance difference between the auxiliary baseline and the task expert is recovered by a merged model. For a model  $m$  and task  $t$ , we define

$$\text{GapClosed}(m, t) = 100 \times \frac{\text{score}(m, t) - s_{\text{aux}}(t)}{s_{\text{expert}}(t) - s_{\text{aux}}(t)}.$$

Under this normalization, 0% corresponds to auxiliary performance and 100% corresponds to expert performance. Values above 100% indicate exceeding the expert, while negative values indicate performance below the auxiliary baseline.

### 3.5 Selector Architecture and Training Details

**Offline classifier.** Our offline selector is a lightweight MLP that takes the similarity features  $\tilde{x}(m_a, m_b, t)$  as input and outputs a categorical distribution over {Linear, SLERP, TIES}. We use a two-layer network with ReLU activations and Adam optimization. We tune basic hyperparameters (hidden width, learning rate, batch size, dropout) on a held-out validation subset of the pairwise merge dataset and use early stopping on validation accuracy.

**Bandit-based selector.** For the online experiments we adopt the neural-linear contextual bandit described in Section 2.3. We instantiate the bandit feature map as a separate MLP encoder  $g_\phi$ , and take  $z(\tilde{x})$  to be its final hidden-layer representation. We warm-start this encoder and the per-operator Bayesian linear models using the training pairwise merge data described in Section 2.3, and then keep the encoder fixed during online adaptation. On top of  $z(\tilde{x})$ , we maintain a Bayesian linear model for each operator and use linear Thompson sampling [Abbasi-Yadkori et al., 2011; Agrawal & Goyal, 2013] as our primary bandit policy, tuning its exploration and regularization hyperparameters on a validation split of the logged data. This policy is then used to select operators when new tasks or models, for instance, a new set of instruct checkpoints are introduced, without retraining the encoder.

## 4 Results

Across code, math, multilingual, and RAG, predictive merge selection consistently improves the trade-off between retaining expert performance and recovering off-domain capability. Section 4.1 shows that in pairwise expert-auxiliary merges, SIMMERGE achieves the strongest overall balance, reducing degradation relative to the expert while improving over auxiliary baselines. Section 4.2 shows that these gains extend to 3-way and 4-way merges, where SIMMERGE continues to outperform fixed operators on both expert-retention and auxiliary-recovery metrics. Because merge operators are not associative, merge order is an additional degree of freedom. Section 4.3 shows that the ordering selected by SIMMERGE yields consistent improvements over random orders. Section 4.4 shows that the same selector trained at 7B transfers to a 111B model without retraining and again achieves the best expert/auxiliary trade-off. Finally, Section 4.5 considers an online setting with distribution shift and shows that a bandit variant learns to select operators efficiently and closely approaches oracle selection.

### 4.1 Learning to Choose the Right Merge Operator in the Pairwise Setting

We begin by examining the fundamental question underlying merge selection: *given two fine-tuned models, can we predict which operator will produce the strongest composite model?* Pairwise (2-way) merges offer the cleanest setting to answer this question and form the basis for training and validating

SIMMERGE. For each task expert and auxiliary checkpoint, we compute pre-merge similarity features, allow SIMMERGE to choose among LINEAR, SLERP, and TIES, and compare the resulting merged model against the three fixed operators. This design isolates the contribution of operator selection, rather than changes in merging mechanics.

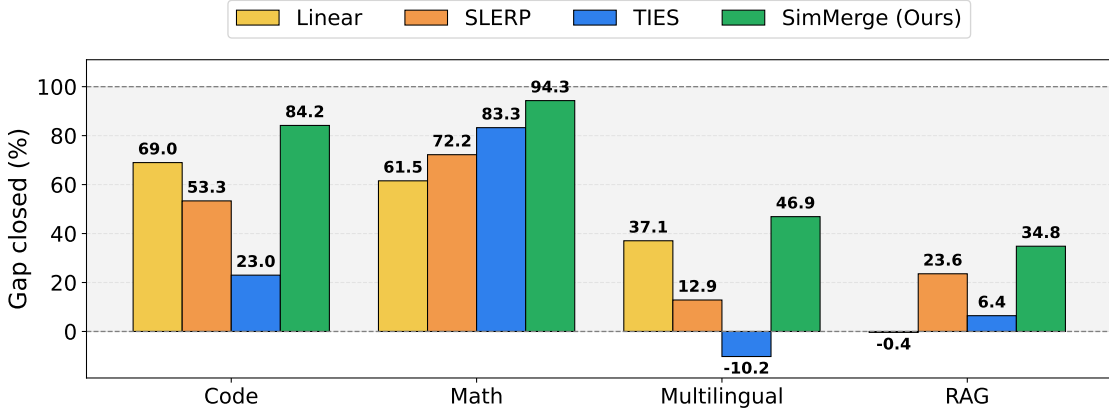


Figure 2: Fraction of the expert–auxiliary performance gap closed by each merge method across Code, Math, Multilingual, and RAG tasks. SimMerge consistently recovers a larger fraction of expert performance than fixed merge operators across all domains.

Figure 2 reports the fraction of the expert-auxiliary performance gap closed by each merge method across Code, Math, Multilingual, and RAG. Overall, the fixed operators exhibit substantial task dependence: an operator that performs well on one domain can be weak, or even harmful on another. For example, Linear is competitive on Code (69.0%) but slightly underperforms the auxiliary baseline on RAG (-0.4%), while TIES is strong on Math (83.3%) yet regresses below the auxiliary baseline on Multilingual (-10.2%). This variability highlights that there is no universally dominant fixed merge rule across domains.

In contrast, SIMMERGE consistently closes the largest fraction of the expert gap in all four domains. On Code, SIMMERGE closes 84.2% of the gap, outperforming the strongest fixed baseline (Linear at 69.0%) by +15.2 percentage points. On Math, SIMMERGE achieves 94.3% gap closed, exceeding all fixed operators (83.3% for TIES, 72.2% for SLERP, 61.5% for Linear), indicating that similarity-driven operator selection can recover near-expert performance in settings where multiple operators are viable but none is reliably optimal.

The Multilingual and RAG results further emphasize robustness. Multilingual is the most challenging domain for fixed operators: Linear closes 37.1% of the gap, SLERP closes 12.9%, and TIES drops below the auxiliary baseline (-10.2%). SIMMERGE reaches 46.9% gap closed, improving over the best fixed baseline (Linear) by +9.8 points and avoiding the severe regressions seen with TIES. On RAG, the gap closed values are lower overall, suggesting a larger remaining discrepancy between merged and expert performance. Still, SIMMERGE achieves the strongest result (34.8%), outperforming SLERP (23.6%) and TIES (6.4%), while Linear slightly underperforms the auxiliary (-0.4%). Macro-averaged across the four domains in Figure 2, SIMMERGE closes 65.0% of the expert-auxiliary gap, compared to 41.8% for the best single fixed operator (Linear); Appendix F.4 reports the calculation. Taken together, these patterns suggest that SIMMERGE not only improves peak performance where fixed operators already work well, but also provides a meaningful robustness advantage on domains where operator choice is harder.

Although SIMMERGE selects only among LINEAR, SLERP, and TIES, it can outperform all three fixed baselines because the fixed operators apply a single rule uniformly across merges, whereas SIMMERGE selects the operator *per instance*. Different expert-auxiliary pairs exhibit varying structural and functional relationships, including parameter alignment, scale differences, sign- and magnitude-based conflict

patterns, functional similarity on probe inputs, and overall parameter geometry that strongly influence which operator succeeds. No single operator handles all such conditions well; however, these properties are reflected in the similarity features observed by SIMMERGE, enabling it to adapt its selection to each pair and approximate the per-instance optimal merge.

Overall, these results show that predictive operator selection based on similarity signals makes merging substantially more reliable than using a single fixed rule. By choosing the operator per expert-auxiliary pair, SIMMERGE avoids large regressions that occur when the wrong operator is applied and consistently recovers a larger fraction of expert performance across domains.

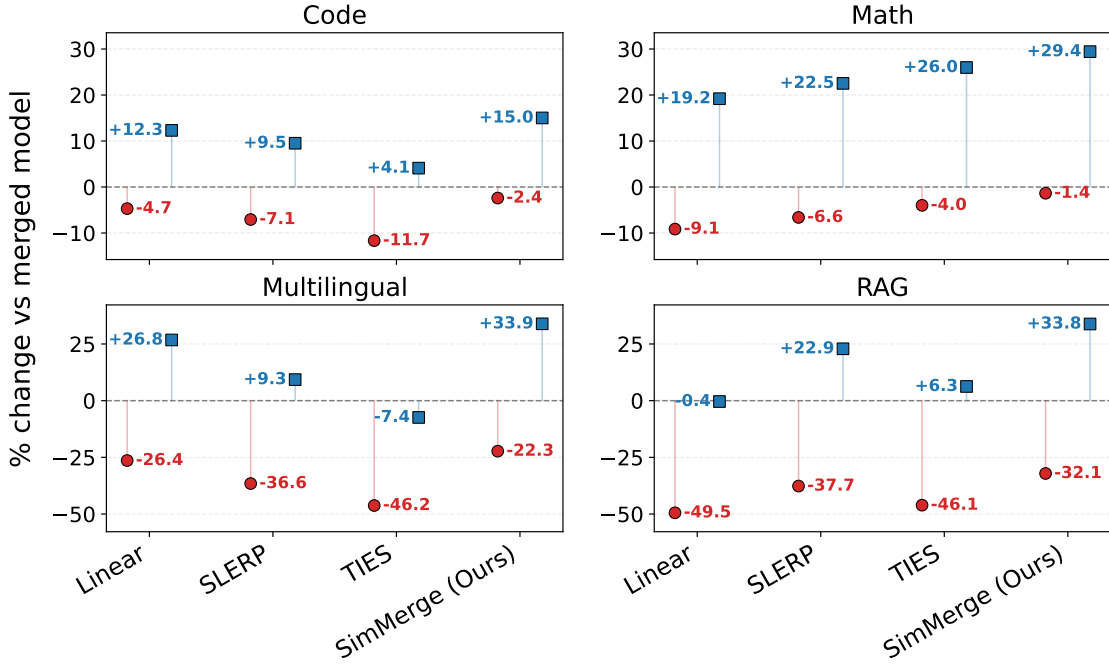


Figure 3: Per-task percentage change in performance for each merge method. Blue markers show  $\Delta_{\text{aux}}$  (change vs. auxiliary; higher is better) and red markers show  $\Delta_{\text{expert}}$  (change vs. task expert; closer to 0 indicates less degradation).

Figure 3 makes this explicit by plotting the normalized percentage change relative to the auxiliary (blue) and the task expert (red). Across all tasks, SIMMERGE achieves the largest gains over the auxiliary model while incurring the smallest degradation relative to the expert. For example, it improves by +29.4% on Math and +33.8% on RAG while degrading by only -1.4% on Math and -2.4% on Code. In contrast, fixed operators show clear trade-offs: LINEAR can approach the expert on some tasks but fails to improve over the auxiliary on RAG, SLERP performs well on Math but weakly elsewhere and TIES even underperforms the auxiliary on Multilingual.

These pairwise results show that similarity-driven operator selection reliably chooses a near-optimal merge rule for each expert-auxiliary pair, producing merged models that consistently improve over the auxiliary baseline while remaining closest to the task expert across all four domains. Appendix G analyzes how similarity signals correlate with outcomes and highlights the performance tails where fixed operators exhibit large regressions, helping explain why per-instance operator selection is critical for robust merging.

## 4.2 From Pairwise Selection to Multi-Way Merges

We next ask whether a selector trained only on 2-way merges can be lifted to the multiway setting. We encode a  $k$ -way merge plan  $\pi$  as an order-aware sequence of pairwise feature blocks  $X(\pi, t)$  and reuse the same similarity encoder and selector architectures to score candidate plans, without any additional  $k$ -way supervision.

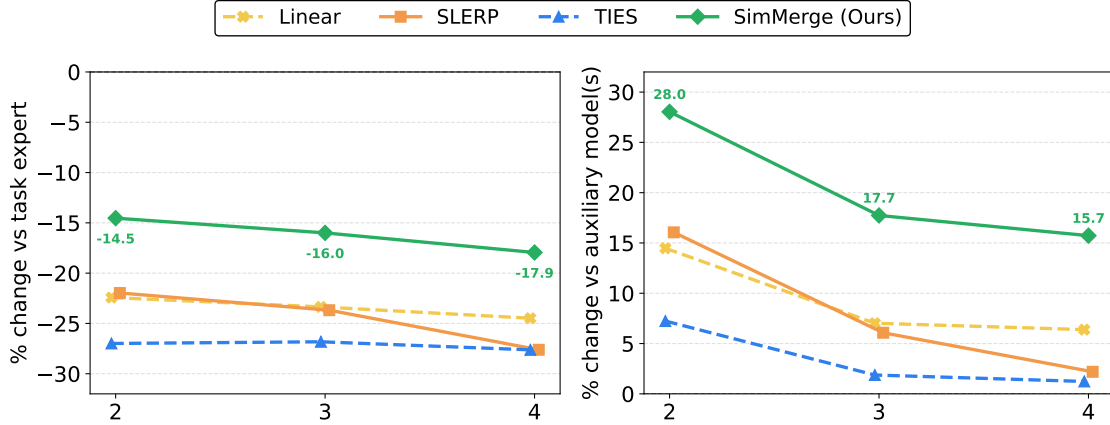


Figure 4: Overall relative performance of 2-, 3-, and 4-way merges, reported as percentage change vs. the task expert (top) and vs. auxiliary models (bottom), macro-averaged over all tasks. SIMMERGE consistently improves over auxiliaries while limiting degradation relative to experts as the number of merged models increases.

Figure 4 summarizes the effect of increasing the number of merged models from  $k = 2$  to  $k = 3$  and  $k = 4$ , macro-averaged over all tasks. The *left* panel shows percentage change in performance relative to the task expert, and the *right* panel shows the corresponding change relative to the auxiliary models. As expected, increasing  $k$  makes merging more challenging for all methods: degradation relative to the expert grows and gains over auxiliaries shrink. Across all values of  $k$ , however, SIMMERGE achieves the best trade-off on both axes. For instance, it stays within  $-14.5\%$  to  $-17.9\%$  of expert performance as  $k$  increases from 2 to 4, while still improving over auxiliaries by  $+28.0\%$ ,  $+17.7\%$ , and  $+15.7\%$  at  $k = 2, 3, 4$ . These results mirror the pairwise trends in Section 4.1 and suggest that similarity-driven selection learned from 2-way merges transfers to multiway merge plans. SIMMERGE remains the best-performing method on both axes across all values of  $k$ . Detailed per-task results for 3- and 4-way merges are provided in Appendix F.2, where we observe the same qualitative behavior across code, math, multilingual, and RAG.

## 4.3 Effect of Merge Order

For 3-way merges, the merge operator is non-associative, so the order in which models are merged can change the final performance. We therefore compare the merge order chosen by our learned selector to a random-order baseline. To isolate the effect of ordering from operator choice, we keep the same sequence of merge operators selected by SIMMERGE fixed and only randomize the permutation of models. This isolates the effect of the merge order itself, independent of the choice of operators.

Figure 5 compares SIMMERGE’s selected order to a random order baseline using the same operator sequence, reported in terms of GAPCLOSED. The numeric labels denote the improvement of the learned ordering over the random baseline. Optimized ordering delivers consistent gains across tasks: SIMMERGE closes a  $+47\%$  gap on Code,  $+16\%$  on Math,  $+11\%$  on Multilingual, and  $+21\%$  on RAG compared to a random ordering. These results indicate that similarity signals are useful not only for selecting merge operators, but also for selecting the merge order, with especially large order effects in Code and RAG.

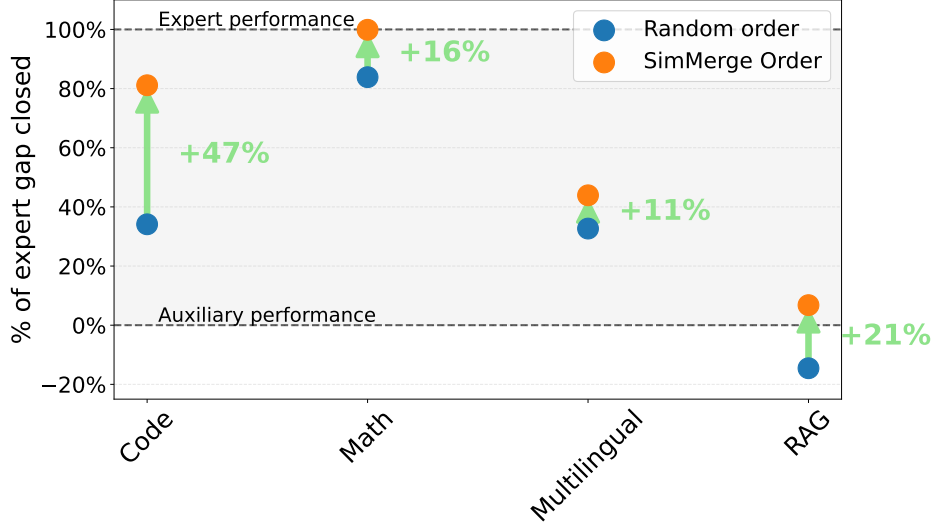


Figure 5: Performance of three-way merges across Code, Math, Multilingual, and RAG tasks, measured as the percentage of the expert–auxiliary performance gap that is closed. Auxiliary performance corresponds to 0%, expert performance to 100%.

#### 4.4 Scaling to a 111B-Parameter Model

To test whether our findings transfer to a substantially larger model, we reuse the selector trained on 7B-parameter checkpoints and repeat the 3-way merging experiments with a 111B-parameter base model, using the same three merge operators and similarity signals as before.

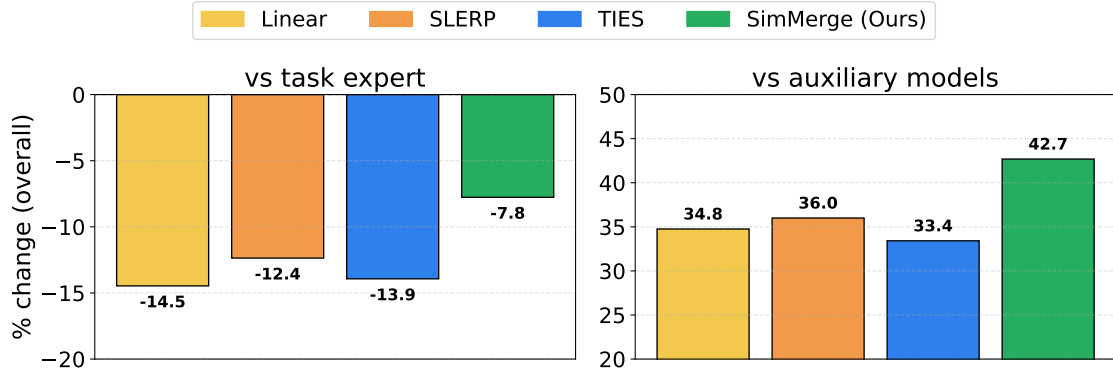


Figure 6: Overall percentage change in performance for 3-way merges on a 111B-parameter model, relative to the task expert (left) and to the auxiliary models (right), macro-averaged over all tasks. Each bar corresponds to using one operator uniformly for all merges; SIMMERGE (green) selects among Linear, SLERP, and TIES using similarity features and yields the smallest degradation relative to the expert and the largest gains over auxiliary models, despite being trained only on 7B-parameter checkpoints.

Figure 6 reports the overall percentage change in performance relative to the task expert (left panel) and to the auxiliary baseline (right panel), averaged over tasks. On the 111B model, SIMMERGE again achieves the best trade-off between expert and auxiliary performance: it reduces degradation relative to the expert to  $-7.8\%$  compared to  $-14.5\%$  (Linear),  $-12.4\%$  (SLERP), and  $-13.9\%$  (TIES). At the same time, it achieves the largest improvement over auxiliary models at  $+42.7\%$  (SIMMERGE) versus  $+34.8\%$  (Linear),  $+36.0\%$  (SLERP), and  $+33.4\%$  (TIES). Appendix F.5 provides a domain-level breakdown for 3-way merges at 111B using both  $\Delta_{\text{expert}}/\Delta_{\text{aux}}$  and GAPCLOSED, and shows the same qualitative pattern across Code, Math, Multilingual, and RAG.

Taken together with the pairwise and multiway results in Sections 4.1 and 4.2, these findings demonstrate that predictive merge selection transfers from 7B to 111B parameters without retraining while providing consistent gains over strong fixed merge operators.

## 4.5 Online Learning

Finally, we evaluate the bandit variant of SIMMERGE in an online setting where the merge operator must be chosen sequentially. At each round the learner observes similarity features for a 3-way merge configuration including an *instruct* checkpoint in addition to the four main tasks and selects one of {Linear, SLERP, TIES}; the reward is the downstream utility of the resulting merge. We compare four policies: (i) a *uniform random* baseline that chooses operators uniformly at random, (ii) a *LinUCB* neural-linear upper-confidence-bound policy, (iii) a *LinTS* neural-linear Thompson-sampling policy (our bandit SIMMERGE), and (iv) an *oracle* that, for each round, plays the best operator in hindsight given full knowledge of all utilities. The oracle is not implementable but serves as an upper bound.

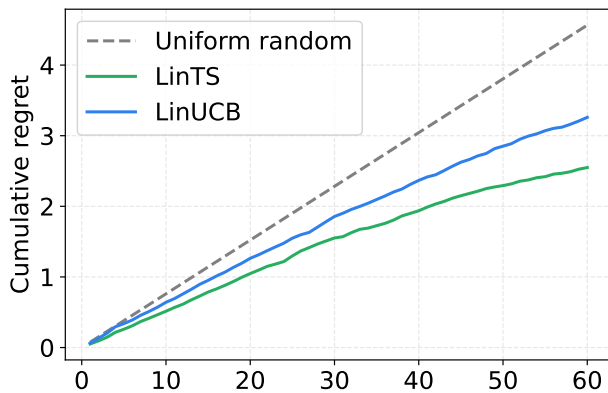


Figure 7: Cumulative regret vs. an oracle policy of 3-way merges. The uniform random baseline accumulates regret nearly linearly. Both neural-linear bandits, LinUCB and LinTS, learn to select better operators, with LinTS achieving consistently lower regret.

Figure 7 shows cumulative regret relative to the oracle over 60 rounds. Uniform random accumulates regret roughly linearly. Both contextual bandits learn quickly and substantially reduce regret, but LinTS dominates LinUCB across the entire horizon: it converges faster and tracks the oracle more closely, indicating that the similarity features are informative enough to support efficient exploration and exploitation for operator selection.

To connect regret to downstream quality, Figure 8 reports the final percentage change in performance for three representative policies: uniform random, LinTS, and oracle, relative to the task expert (left) and to the auxiliary baseline (right), aggregated over 3-way merges on Code, Math, Multilingual, RAG, Instruct, and the overall macro-average. LinTS closely tracks the oracle on both axes and consistently improves over the uniform random baseline. For example, on the overall macro-average it reaches  $-18.8\%$  relative to the expert while improving by  $+13.7\%$  over the auxiliary baseline. These results show that the same similarity features can support a practical online policy via Thompson sampling, enabling adaptation to distribution shift while retaining much of the benefit of full-information operator choice.

## 5 Related Work

**Weight-space model merging.** A large body of work studies how to combine models directly in parameter space. The most common setting assumes experts fine-tuned from a shared base checkpoint

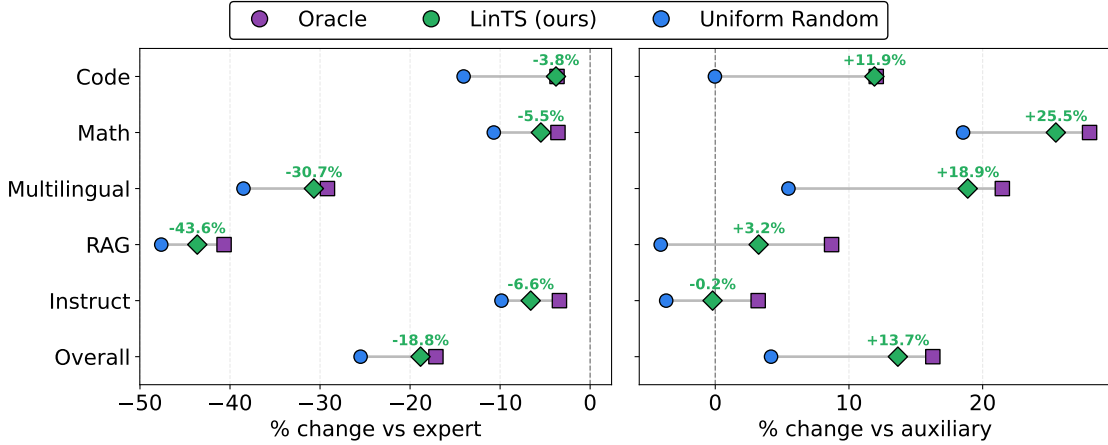


Figure 8: Percentage change in performance for 3-way merges under three online policies, relative to the task expert (left) and to auxiliary models (right), across code, math, multilingual, RAG, instruct, and the overall average. The oracle chooses the best operator per round. LinTS (our bandit SIMMERGE) closely matches the oracle and consistently outperforms the uniform random baseline, achieving smaller degradation vs. experts and larger gains vs. auxiliaries.

and merges them by simple or weighted averaging in weight space or task-vector space [Matena & Raffel, 2021; Ilharco et al., 2023; Yadav et al., 2023]. Other lines handle models with different initializations via permutation-alignment and subspace-matching techniques [Entezari et al., 2022; Ainsworth et al., 2022]. Merging has also been explored for parameter-efficient adaptation [Houlsby et al., 2019], LoRA [Hu et al., 2022], LEGO [Zhao et al., 2025] and at inference time via soft ensembles or routing [Muqeeth et al., 2023]. These methods are largely *operator-centric*: they propose new rules for how to interpolate or combine parameters, often with improved robustness or interference control, but they typically assume that a single merge rule is applied uniformly across all model pairs.

**Interference-aware and geometry-aware operators.** Within the shared-checkpoint regime that we also study, several works design more sophisticated merge operators. Task arithmetic [Ilharco et al., 2023] introduces task vectors and shows that linear combinations can add or negate properties. Fisher-weighted averaging [Matena & Raffel, 2022] weights parameters by estimated importance from Fisher information. TIES [Yadav et al., 2023] and DARE [Yu et al., 2024] prune or reweight task vectors to reduce destructive interference before merging, while SLERP [Shoemaker, 1985] follows spherical geodesics in weight or task-vector space. Recent work also explores structured or alignment-based rules and subspace matching [Tam et al., 2023; Stoica et al., 2024; Huang et al., 2024], and open-source toolkits such as MergeKit [Goddard et al., 2024] have made these operators widely accessible. In all of these cases, however, the practitioner must still choose which operator, hyperparameters, order or subset of models to apply for a given use case.

**Automating merge hyperparameters.** Closer to our goal are methods that tune merge hyperparameters rather than the base operator itself. Fisher merging [Matena & Raffel, 2022] uses data-derived Fisher information to compute a weighted average. AdaMerge [Yang et al., 2024] chooses task-vector coefficients to minimize merge-model entropy on unlabeled data. Akiba et al. [2025] apply evolutionary search to optimize merge recipes, iteratively refining coefficients and layer-wise schedules. These approaches still operate within a fixed operator family and typically require multiple merge-and-evaluate steps per configuration.

In contrast, our work does not propose a new merge rule or a new way to set its continuous hyperparameters. Instead, we treat *merge selection* itself as the learning problem. We train a lightweight selector that uses inexpensive model similarity signals to choose between Linear, SLERP, and TIES and to predict the

merge order that performs best for a given set of checkpoints on a target task. At test time, SIMMERGE replaces an exhaustive merge-and-evaluate loop with a single forward pass of this selector and a single merge. Unlike prior hyperparameter-search methods, our selector is trained once on 2-way merges and then reused for multiway planning and for larger models, and our neural linear bandit [Riquelme et al., 2018] variant supports online adaptation as new tasks, models, or operators are introduced.

## 6 Conclusion

Model merging is a promising alternative to joint training and large ensembles, but its reliability often depends on selecting the merge operator and, for multiway merges, the merge order. We introduced SIMMERGE, a predictive merge selection framework that uses pre-merge similarity signals from model weights and unlabeled probes to choose merge configurations without costly merge-and-evaluate loops.

Across pairwise and multiway merges of 7B checkpoints in code, math, multilingual and retrieval-augmented generation, SIMMERGE consistently outperforms fixed operators by selecting operators per instance and choosing effective merge orders when operators are non-associative. The same selector transfers to multiway merges and 111B models without retraining, improving the expert-auxiliary trade-off while reducing expert degradation. An online neural-linear bandit variant further adapts under partial feedback as tasks and model pools shift.

These results suggest a simple takeaway: reliable model composition is not only about designing better merge rules, but also about learning when to apply the ones we already have. Predictive merge selection turns large checkpoint catalogs into practical, on-demand building blocks under tight evaluation budgets, and it naturally extends as new operators and new model families become available. Future work can expand the operator set, improve intermediate-metric propagation for deeper merge trees, and explore task-agnostic selection that generalizes across evaluation suites with minimal calibration.

## References

Yasin Abbasi-Yadkori, Dávid Pál, and Csaba Szepesvári. Improved algorithms for linear stochastic bandits. In *Advances in Neural Information Processing Systems*, volume 24, 2011.

Shipra Agrawal and Navin Goyal. Thompson sampling for contextual bandits with linear payoffs. In *Proceedings of the 30th International Conference on Machine Learning*, pp. 127–135. PMLR, 2013.

Samuel K. Ainsworth, Jonathan Hayase, and Siddhartha Srinivasa. Git re-basin: Merging models modulo permutation symmetries. *arXiv preprint arXiv:2209.04836*, 2022. URL <https://arxiv.org/abs/2209.04836>.

Takuya Akiba, Makoto Shing, Yujin Tang, Qi Sun, and David Ha. Evolutionary optimization of model merging recipes. *arXiv preprint arXiv:2403.13187*, 2024. URL <https://arxiv.org/abs/2403.13187>.

Takuya Akiba, Makoto Shing, Yujin Tang, Qi Sun, and David Ha. Evolutionary optimization of model merging recipes. *Nature Machine Intelligence*, 7(2):195–204, 2025.

Stephen Boyd and Lieven Vandenberghe. *Convex Optimization*. Cambridge University Press, 2004.

Mark Chen. Evaluating large language models trained on code. *arXiv preprint arXiv:2107.03374*, 2021.

Karl Cobbe, Vineet Kosaraju, Mohammad Bavarian, Mark Chen, Heewoo Jun, Lukasz Kaiser, Matthias Plappert, Jerry Tworek, Jacob Hilton, Reiichiro Nakano, Christopher Hesse, and John Schulman. Training verifiers to solve math word problems. *arXiv preprint arXiv:2110.14168*, 2021.

Team Cohere, Arash Ahmadian, Marwan Ahmed, Jay Alammar, Milad Alizadeh, Yazeed Alnumay, Sophia Althammer, Arkady Arkhangorodsky, Viraat Aryabumi, Dennis Aumiller, et al. Command-A: An enterprise-ready large language model. *arXiv preprint arXiv:2504.00698*, 2025.

Thomas M. Cover and Joy A. Thomas. *Elements of Information Theory*. Wiley, 2 edition, 2006.

Imre Csiszár. Information-type measures of difference of probability distributions and indirect observation. *Studia Sci. Math. Hungarica*, 2:299–318, 1967.

Rahim Entezari, Hanie Sedghi, Olga Saukh, and Behnam Neyshabur. The role of permutation invariance in linear mode connectivity of neural networks. In *International Conference on Learning Representations*, 2022.

Charles Goddard, Shamane Siriwardhana, Malikeh Ehghaghi, Luke Meyers, Vlad Karpukhin, Brian Benedict, Mark McQuade, and Jacob Solawetz. Arcee’s MergeKit: A toolkit for merging large language models. *arXiv preprint arXiv:2403.13257*, 2024. URL <https://arxiv.org/abs/2403.13257>.

Dan Hendrycks, Collin Burns, Saurav Kadavath, Akul Arora, Steven Basart, Eric Tang, Dawn Song, and Jacob Steinhardt. Measuring mathematical problem solving with the math dataset. *arXiv preprint arXiv:2103.03874*, 2021.

Neil Houlsby, Andrei Giurgiu, Stanislaw Jastrzebski, Bruna Morrone, Quentin de Laroussilhe, Andrea Gesmundo, Mona Attariyan, and Sylvain Gelly. Parameter-efficient transfer learning for NLP. In *International Conference on Machine Learning (ICML)*, volume 97, pp. 2790–2799. PMLR, 2019. URL <https://proceedings.mlr.press/v97/houlsby19a.html>.

Edward J. Hu, Yelong Shen, Phillip Wallis, Zeyuan Allen-Zhu, Yuanzhi Li, Shean Wang, Lu Wang, and Weizhu Chen. Lora: Low-rank adaptation of large language models. In *International Conference on Learning Representations (ICLR)*, 2022. URL <https://openreview.net/forum?id=nZeVKeeFYf9>.

Chaoyue Huang, Xiangyu Yue, et al. Emr-merging: Tuning-free high-performance model merging. In *Advances in Neural Information Processing Systems (NeurIPS)*, 2024. URL <https://arxiv.org/abs/2405.17461>.

Gabriel Ilharco, Marco Túlio Ribeiro, Mitchell Wortsman, Ludwig Schmidt, Hannaneh Hajishirzi, and Ali Farhadi. Editing models with task arithmetic. In *The Eleventh International Conference on Learning Representations*, 2023.

Jiawei Liu, Chunqiu Steven Xia, Yuyao Wang, and Lingming Zhang. Is your code generated by ChatGPT really correct? rigorous evaluation of large language models for code generation. *Advances in Neural Information Processing Systems*, 36:21558–21572, 2023.

Michael Matena and Colin Raffel. Merging models with fisher-weighted averaging. *arXiv preprint arXiv:2111.09832*, 2021. URL <https://arxiv.org/abs/2111.09832>.

Michael Matena and Colin Raffel. Merging models with fisher-weighted averaging. In *Advances in Neural Information Processing Systems (NeurIPS)*, 2022. URL <https://arxiv.org/abs/2111.09832>.

Mohammed Muqeeth, Haokun Liu, and Colin Raffel. Soft merging of experts with adaptive routing. *arXiv*, abs/2306.03745, 2023.

Shishir G. Patil, Huanzhi Mao, Charlie Cheng-Jie Ji, Fanjia Yan, Vishnu Suresh, Ion Stoica, and Joseph E. Gonzalez. The berkeley function calling leaderboard (bfcl): From tool use to agentic evaluation of large language models. In *Forty-second International Conference on Machine Learning*, 2025.

Carlos Riquelme, George Tucker, and Jasper Snoek. Deep bayesian bandits showdown: An empirical comparison of bayesian deep networks for thompson sampling. *arXiv preprint arXiv:1802.09127*, 2018. URL <https://arxiv.org/abs/1802.09127>.

Freda Shi, Mirac Suzgun, Markus Freitag, Xuezhi Wang, Suraj Srivats, Soroush Vosoughi, Hyung Won Chung, Yi Tay, Sebastian Ruder, Denny Zhou, et al. Language models are multilingual chain-of-thought reasoners. *arXiv preprint arXiv:2210.03057*, 2022.

Ken Shoemake. Animating rotation with quaternion curves. In *SIGGRAPH '85: Proceedings of the 12th Annual Conference on Computer Graphics and Interactive Techniques*, pp. 245–254. ACM, 1985. doi: 10.1145/325165.325242. URL <https://dl.acm.org/doi/10.1145/325165.325242>.

George Stoica, Daniel Bolya, Jakob Bjorner, Pratik Ramesh, Taylor Hearn, and Judy Hoffman. Zipit! merging models from different tasks without training. In *International Conference on Learning Representations (ICLR)*, 2024. URL <https://openreview.net/forum?id=LEYUkvdUhq>.

Derek Tam, Mohit Bansal, and Colin Raffel. Merging by matching models in task parameter subspaces. *arXiv preprint arXiv:2312.04339*, 2023. URL <https://arxiv.org/abs/2312.04339>.

Mitchell Wortsman, Gabriel Ilharco, Samir Yitzhak Gadre, Rebecca Roelofs, Raphael Gontijo-Lopes, Ari S. Morcos, Hongseok Namkoong, Ali Farhadi, Yair Carmon, Simon Kornblith, and Ludwig Schmidt. Model soups: averaging weights of multiple fine-tuned models improves accuracy without increasing inference time. In *International Conference on Machine Learning (ICML)*, volume 162, pp. 23965–23998. PMLR, 2022. URL <https://proceedings.mlr.press/v162/wortsman22a.html>.

Prateek Yadav, Derek Tam, Leshem Choshen, Colin Raffel, and Mohit Bansal. Ties-merging: Resolving interference when merging models. *arXiv preprint arXiv:2306.01708*, 2023. URL <https://arxiv.org/abs/2306.01708>.

Enneng Yang, Zhenyi Wang, Li Shen, Shiwei Liu, Guibing Guo, Xingwei Wang, and Dacheng Tao. Adamerging: Adaptive model merging for multi-task learning. In *The Twelfth International Conference on Learning Representations*, 2024.

Shunyu Yao, Noah Shinn, Pedram Razavi, and Karthik R. Narasimhan. tau-bench: A benchmark for tool-agent-user interaction in real-world domains. In *International Conference on Learning Representations (ICLR)*, 2025. URL <https://openreview.net/forum?id=roNSXZpUDN>.

Le Yu, Bowen Yu, Haiyang Yu, Fei Huang, and Yongbin Li. Language models are super mario: Absorbing abilities from homologous models as a free lunch. In *Forty-first International Conference on Machine Learning*, 2024.

Zhongshen Zeng, Pengguang Chen, Shu Liu, Haiyun Jiang, and Jiaya Jia. Mr-gsm8k: A meta-reasoning benchmark for large language model evaluation. *arXiv preprint arXiv:2312.17080*, 2023.

Ziyu Zhao, Tao Shen, Didi Zhu, Zexi Li, Jing Su, Xuwu Wang, and Fei Wu. Merging loras like playing lego: Pushing the modularity of lora to extremes through rank-wise clustering. In *The Thirteenth International Conference on Learning Representations*, 2025.

Jeffrey Zhou, Tianjian Lu, Swaroop Mishra, Siddhartha Brahma, Sujoy Basu, Yi Luan, Denny Zhou, and Le Hou. Instruction-following evaluation for large language models. *arXiv preprint arXiv:2311.07911*, 2023.

## A Merge Operators

This appendix specifies the merge operators used in the main text: linear interpolation (LINEAR), spherical linear interpolation (SLERP), and a TIES-style sign-consistent merge (TIES). All operators act on corresponding parameter tensors of two models  $m_a$  and  $m_b$  with flattened parameters  $\theta_1 = \theta(m_a), \theta_2 = \theta(m_b) \in \mathbb{R}^d$ . Unless stated otherwise, we use a fixed mixing coefficient  $\alpha = 0.5$  in the experiments.

### A.1 Linear Interpolation

Linear interpolation (LINEAR) combines parameters by a convex combination,

$$M_{\text{Lin}}(\theta_1, \theta_2; \alpha) = (1 - \alpha)\theta_1 + \alpha\theta_2.$$

In practice we apply this operation layerwise on each parameter tensor such as attention and MLP weights and biases. We do not apply any additional rescaling beyond the convex weights.

### A.2 Spherical Linear Interpolation (SLERP)

Spherical linear interpolation (SLERP) [Shoemake, 1985] interpolates on the unit sphere in parameter space, preserving the norms of the inputs. For each layer we normalize

$$\hat{\theta}_i = \frac{\theta_i}{\|\theta_i\|_2}, \quad i \in \{1, 2\},$$

compute the angle  $\varphi = \arccos(\hat{\theta}_1 \cdot \hat{\theta}_2)$  and form the spherical interpolation

$$\tilde{\theta}_{\text{unit}} = \frac{\sin((1 - \alpha)\varphi)}{\sin \varphi} \hat{\theta}_1 + \frac{\sin(\alpha\varphi)}{\sin \varphi} \hat{\theta}_2.$$

We then rescale  $\tilde{\theta}_{\text{unit}}$  to match the average input norm,

$$\tilde{\theta} = \frac{\|\theta_1\|_2 + \|\theta_2\|_2}{2} \cdot \frac{\tilde{\theta}_{\text{unit}}}{\|\tilde{\theta}_{\text{unit}}\|_2}.$$

The normalization and rescaling are applied per layer, using the layerwise parameter tensors. This follows the standard SLERP construction and keeps parameter magnitudes comparable across merges.

### A.3 TIES-Style Sign-Consistent Merge

The TIES-merging (TRIM, ELECT SIGN and MERGE) [Yadav et al., 2023] is a sign-consistent rule that suppresses conflicting updates while interpolating non-conflicting entries. We abstract it as

$$M_{\text{TIES}}(\theta_1, \theta_2; \alpha) = T_\tau(\theta_1, \theta_2; \alpha),$$

where  $\tau \geq 0$  is a threshold hyperparameter.

Let  $\theta_1[j], \theta_2[j]$  denote the  $j$ -th coordinate of the two parameter vectors. The operator  $T_\tau$  is defined coordinate-wise:

$$T_\tau(\theta_1, \theta_2; \alpha)[j] = \begin{cases} \alpha \theta_1[j] + (1 - \alpha) \theta_2[j], & \text{if } \theta_1[j]\theta_2[j] > 0 \text{ and } \max(|\theta_1[j]|, |\theta_2[j]|) \geq \tau, \\ \theta_1[j], & \text{if } \theta_1[j]\theta_2[j] \leq 0 \text{ and } |\theta_1[j]| \geq |\theta_2[j]| \text{ and } |\theta_1[j]| \geq \tau, \\ \theta_2[j], & \text{if } \theta_1[j]\theta_2[j] \leq 0 \text{ and } |\theta_2[j]| > |\theta_1[j]| \text{ and } |\theta_2[j]| \geq \tau, \\ 0, & \text{otherwise.} \end{cases}$$

Thus, coordinates with aligned sign and sufficient magnitude are interpolated linearly, while coordinates with sign conflicts are resolved by selecting the larger-magnitude entry, and small-magnitude coordinates are pruned. In our implementation,  $T_\tau$  is applied layerwise to each parameter tensor, and the same threshold  $\tau$  is used across layers. The value of  $\tau$  is treated as a hyperparameter and tuned on the pairwise validation split.

## B Similarity Metrics and Feature Construction

This appendix specifies the similarity metrics and the construction of the feature vectors  $x(m_a, m_b, t)$  and  $\tilde{x}(m_a, m_b, t)$  used by SIMMERGE.

### B.1 Probe Data and Notation

For each task  $t \in \mathcal{T}$  we draw an unlabeled probe set  $\mathcal{P}_t = \{x_1, \dots, x_{N_t}\}$  from the input distribution of  $t$ . No labels are used in any similarity metric.

For a model  $m$  and a prompt  $x$ , let  $z_m(x)$  denote the logits produced under teacher forcing. At each decoding position  $j$  (token index), we write

$$p_m(\cdot | x, j) = \text{softmax}(z_m(x)_j)$$

for the next-token predictive distribution over the vocabulary. For transformer activations, let  $h_m^{(\ell)}(x) \in \mathbb{R}^{T \times d_\ell}$  denote the post-residual hidden states at layer  $\ell$ , where  $T$  is the sequence length. When needed, we flatten  $h_m^{(\ell)}(x)$  across sequence positions into a single vector in  $\mathbb{R}^{T d_\ell}$ . Equivalently, we concatenate token representations.

For attention patterns, let  $A_m^{(\ell, h)}(x) \in \mathbb{R}^{T \times T}$  denote the attention weight matrix (softmax over keys) at layer  $\ell$  and head  $h$  for prompt  $x$ .

For each model  $m$  we denote its flattened parameter vector by  $\theta(m) \in \mathbb{R}^d$ . For brevity, we write  $\theta_a = \theta(m_a)$  and  $\theta_b = \theta(m_b)$ .

### B.2 Data-Based Metrics

Data-based metrics compare model behavior on the probe set  $\mathcal{P}_t$ .

**KL divergence between predictive distributions.** For an ordered pair  $(m_a, m_b)$ , prompt  $x \in \mathcal{P}_t$ , and position  $j$ , the pointwise KL divergence is

$$D_{\text{KL}}(p_a(\cdot | x, j) \| p_b(\cdot | x, j)) = \sum_i p_a(i | x, j) \log \frac{p_a(i | x, j)}{p_b(i | x, j)}.$$

We average over positions and prompts to obtain

$$\text{KL}_{\text{mean}}(m_a, m_b, t) = \frac{1}{N_t} \sum_{x \in \mathcal{P}_t} \frac{1}{|J(x)|} \sum_{j \in J(x)} D_{\text{KL}}(p_a(\cdot | x, j) \| p_b(\cdot | x, j)),$$

where  $J(x)$  is the set of teacher-forced positions used for evaluation. We additionally record robust summary statistics over prompts (median and empirical quantiles, such as 25th/75th/90th percentiles). KL is computed in log-space with standard numerical stabilization.

**Activation cosine similarity.** For each layer  $\ell$  and prompt  $x \in \mathcal{P}_t$ , let  $\text{vec}(h_m^{(\ell)}(x)) \in \mathbb{R}^{T d_\ell}$  denote the flattened hidden states. We define

$$\cos_h^{(\ell)}(m_a, m_b, x) = \frac{\langle \text{vec}(h_a^{(\ell)}(x)), \text{vec}(h_b^{(\ell)}(x)) \rangle}{\|\text{vec}(h_a^{(\ell)}(x))\|_2 \|\text{vec}(h_b^{(\ell)}(x))\|_2}, \quad \cos_h^{(\ell)}(m_a, m_b, t) = \frac{1}{N_t} \sum_{x \in \mathcal{P}_t} \cos_h^{(\ell)}(m_a, m_b, x).$$

We keep either the full per-layer sequence  $\{\cos_h^{(\ell)}\}_{\ell=1}^L$  for later summarization or aggregate across layers immediately.

**Attention-pattern cosine similarity.** For each layer  $\ell$ , head  $h$ , and prompt  $x \in \mathcal{P}_t$ , we flatten attention matrices and compute

$$\cos_A^{(\ell,h)}(m_a, m_b, x) = \frac{\langle \text{vec}(A_a^{(\ell,h)}(x)), \text{vec}(A_b^{(\ell,h)}(x)) \rangle}{\|\text{vec}(A_a^{(\ell,h)}(x))\|_2 \|\text{vec}(A_b^{(\ell,h)}(x))\|_2}.$$

We summarize these values across prompts, heads, and layers using the same robust statistics as above (mean/median/quantiles), yielding a compact set of attention-similarity features.

### B.3 Weight-Based Metrics

Weight-based metrics compare parameters directly and do not depend on  $\mathcal{P}_t$ .

**Weight cosine similarity.** For flattened parameter vectors  $\theta_a, \theta_b \in \mathbb{R}^d$ ,

$$\cos_W(m_a, m_b) = \frac{\langle \theta_a, \theta_b \rangle}{\|\theta_a\|_2 \|\theta_b\|_2}.$$

We optionally compute layerwise or module-restricted variants by restricting  $\theta_a, \theta_b$  to parameters of a given transformer block or to attention/MLP submodules.

**Weight  $\ell_2$  distance.**

$$d_W(m_a, m_b) = \|\theta_a - \theta_b\|_2,$$

again optionally computed per-layer or per-module by restriction to parameter subsets.

**Weight norms.** We record  $\|\theta_a\|_2$  and  $\|\theta_b\|_2$  (and optionally their layerwise/modulewise norms) to capture global scale differences that can interact with merge behavior.

### B.4 Feature Vector Construction

Each metric yields either a scalar or a short sequence indexed by layers and, for attention, optionally heads. To obtain a fixed-dimensional representation, sequence-valued metrics are summarized using robust statistics such as the mean, median, and selected quantiles, and all summaries are concatenated into a single feature vector

$$x(m_a, m_b, t) \in \mathbb{R}^m.$$

By default, we append an explicit task encoding  $c(t) \in \mathbb{R}^{d_c}$  and use

$$\tilde{x}(m_a, m_b, t) = x(m_a, m_b, t) \oplus c(t) \in \mathbb{R}^{m+d_c}$$

as the input to all learned components. We also evaluate a task-agnostic variant that omits  $c(t)$ ; the comparison is reported in Appendix F.1. The improvement from the task encoding is modest but consistent, so we keep it enabled in the main experiments.

## C Why Pairwise Training Can Transfer to Multi-Way Planning

This section provides intuition for why a scorer trained using pairwise-derived signals can be effective for ranking multi-way merge plans. For a  $k$ -way plan  $\pi = (m_{i_1} \rightarrow \dots \rightarrow m_{i_k})$  on task  $t$ , SIMMERGE represents the plan by concatenating step-wise feature blocks,

$$X(\pi, t) = [x(m_{i_1}, m_{i_2}, t), \dots, x(m_{i_{k-1}}, m_{i_k}, t)] \oplus c(t).$$

This construction is motivated by the observation that non-associativity makes the *local* interaction between consecutive merge steps consequential: changing the order changes which pairs interact early versus late, and these interactions are reflected in the corresponding pairwise similarity regimes.

A sufficient condition for this representation to be useful is that the utility of executing a plan,  $U(\pi, t)$ , depends smoothly on (or can be well-approximated by) a low-order function of these step-wise interactions. For example, if

$$U(\pi, t) \approx \sum_{s=1}^{k-1} \psi(x(m_{i_s}, m_{i_{s+1}}, t), t)$$

for some unknown function  $\psi$ , then a learned plan scorer can estimate  $U(\pi, t)$  from  $X(\pi, t)$  by aggregating step-wise contributions. More generally, if  $U(\pi, t) = F(x_1, \dots, x_{k-1}, c(t))$  is a sufficiently smooth function of the step blocks  $x_s$ , then a first-order expansion around typical interaction regimes yields an approximately additive dependence on the concatenated features. This motivates learning  $f_{\text{plan}}$  on plan representations built from the same pairwise feature blocks used for operator selection.

## D Propagation of Similarity Metrics to Multi-Way Plans

This appendix details how we construct approximate similarity features for intermediate steps when scoring multi-way merge plans, without explicitly constructing and evaluating intermediate merged parameters for each candidate plan.

A multi-way plan involves intermediate merged checkpoints. To score candidate plans efficiently, we use a *proxy* representation for an intermediate step formed by merging  $a$  and  $b$  with coefficient  $\alpha$ . In the main experiments we fix  $\alpha = \frac{1}{2}$  and treat the intermediate as an equal-weight combination for the purpose of constructing features. For data-based quantities such as KL, where the intermediate model's predictive distribution is not available without executing the merge, we use mixture-inspired proxy estimates derived from standard inequalities; these values serve as inexpensive features rather than exact measurements of the true intermediate model.

Orientation is explicit because some metrics are asymmetric (notably KL). We write

$$(a+b, c) : \quad G_L = (1-\alpha)P_a + \alpha P_b, \quad G_R = P_c, \quad \text{and} \quad (c, a+b) : \quad G_L = P_c, \quad G_R = (1-\alpha)Q_a + \alpha Q_b,$$

where  $P_\cdot$  and  $Q_\cdot$  denote predictive distributions on the probe set or distributional proxies derived from logits.

### D.1 KL Divergence Proxies

By the log-sum inequality and the joint convexity of KL (more generally,  $f$ -divergences) in each argument [Csiszár, 1967; Cover & Thomas, 2006],

$$\text{KL}((1-\alpha)P_a + \alpha P_b \parallel P_c) \leq (1-\alpha) \text{KL}(P_a \parallel P_c) + \alpha \text{KL}(P_b \parallel P_c), \quad (1)$$

$$\text{KL}(P_c \parallel (1-\alpha)Q_a + \alpha Q_b) \leq (1-\alpha) \text{KL}(P_c \parallel Q_a) + \alpha \text{KL}(P_c \parallel Q_b). \quad (2)$$

More generally, when both arguments are mixtures,

$$G_L := \sum_i w_i P_i, \quad G_R := \sum_j v_j Q_j,$$

with  $w_i, v_j \geq 0$  and  $\sum_i w_i = \sum_j v_j = 1$ , we have

$$\text{KL}(G_L \| G_R) \leq \sum_{i,j} w_i v_j \text{KL}(P_i \| Q_j).$$

In practice, we use the right-hand sides of (1) and (2) as propagated *proxy* values.

## D.2 $\ell_2$ Parameter Distance Proxies

Let  $\theta_a, \theta_b, \theta_c \in \mathbb{R}^d$  be flattened parameter vectors and  $L_2(\theta, \theta') = \|\theta - \theta'\|_2$ . By the triangle inequality and positive homogeneity of norms [Boyd & Vandenberghe, 2004],

$$\|(1 - \alpha)\theta_a + \alpha\theta_b - \theta_c\|_2 \leq (1 - \alpha) \|\theta_a - \theta_c\|_2 + \alpha \|\theta_b - \theta_c\|_2, \quad (3)$$

$$\|\theta_c - ((1 - \alpha)\theta_a + \alpha\theta_b)\|_2 \leq (1 - \alpha) \|\theta_c - \theta_a\|_2 + \alpha \|\theta_c - \theta_b\|_2. \quad (4)$$

We use the right-hand sides as propagated proxy values and mark them *proxy upper*.

## D.3 Cosine Similarity Proxies (Weights or Attention Patterns)

Define  $\cos(u, v) = \frac{\langle u, v \rangle}{\|u\|_2 \|v\|_2}$ . Because the denominator is nonlinear in mixtures, an exact cosine with an intermediate proxy would require dot products and norms that are typically not logged for every possible intermediate. We therefore use a simple, stable proxy:

$$\cos((1 - \alpha)u_a + \alpha u_b, u_c) \approx (1 - \alpha) \cos(u_a, u_c) + \alpha \cos(u_b, u_c), \quad (5)$$

and similarly for  $\cos(u_c, (1 - \alpha)u_a + \alpha u_b)$ . We clip the resulting values to  $[-1, 1]$ . This rule is used both for weight-vector cosines (with  $u. = \theta.$ ) and for attention-pattern cosines (with  $u. = \text{vec}(A^{(\ell, h)}(x))$  after summarization).

These propagated proxy values are aggregated using the same robust statistics as in Appendix B and inserted into the plan representation  $X(\pi, t)$  whenever a similarity involving an intermediate step is required. This allows SIMMERGE to score candidate multi-step merge sequences using a precomputed pairwise similarity table, without recomputing similarities for every hypothetical intermediate merge.

## E Evaluation Benchmarks and Metrics

We provide additional details on the benchmarks and evaluation metrics used for each task domain.

**Math reasoning.** We evaluate mathematical reasoning on *MATH* [Hendrycks et al., 2021] and *GSM8K* [Cobbe et al., 2021]. Both benchmarks consist of grade-school to competition-level math problems that require multi-step reasoning and symbolic manipulation. Models are evaluated using *exact match* accuracy, where a prediction is considered correct only if the final answer exactly matches the reference solution. For *GSM8K*, answers are normalized following standard evaluation protocols to account for formatting differences.

**Multilingual question answering.** Multilingual performance is measured using an internal multilingual QA suite together with *MGSM* [Shi et al., 2022], which extends GSM-style math reasoning to multiple languages. MGSM evaluates cross-lingual generalization and reasoning robustness. Performance is reported using accuracy and win-rate metrics, where win-rate measures the fraction of examples on which a model’s answer is preferred over a baseline under automatic or human evaluation, depending on the benchmark. These metrics capture both correctness and relative answer quality across languages.

**Code generation.** Code generation is evaluated on *HumanEval\_Python* [Chen, 2021] and *MBPP+* [Liu et al., 2023]. Both benchmarks assess functional correctness of generated programs against unit tests. We report *pass@1*, which measures the probability that the first generated solution passes all test cases. This metric reflects single-sample code generation quality and is standard in code evaluation.

**Retrieval-augmented generation (RAG).** RAG performance is evaluated on *TauBench* [Yao et al., 2025] and *BFCL* [Patil et al., 2025], which test a model’s ability to integrate retrieved evidence into accurate responses. We report accuracy and F1 score, depending on the benchmark, following their official evaluation protocols. These metrics assess both answer correctness and overlap with reference responses, capturing retrieval grounding quality.

**Instruction following.** For instruction-following experiments used in the bandit setting, we evaluate on *IFEval* [Zhou et al., 2023]. IFEval measures a model’s ability to follow explicit instructions and constraints. Performance is reported using the benchmark’s standard instruction-compliance score, which aggregates binary success indicators across multiple instruction types.

All evaluations are run three times with different random seeds, and we report the mean score. This reduces variance due to stochastic decoding and ensures stable comparisons across merge methods.

## F Additional Results

### F.1 Classifier Accuracy and Task-Encoding Ablation

To quantify predictive accuracy, we report confusion matrices for the offline selector on the held-out pairwise test set of 60 merges. We compare our default task-conditioned representation, which appends a task encoding  $c(t)$  to the similarity features, against a task-agnostic variant that omits  $c(t)$ .

Figure 9 shows that task conditioning yields a small but consistent improvement across all classes. With the task encoding, the selector correctly identifies Linear in 87.5% of cases, SLERP in 82.8%, and TIES in 68.2%. Without the task encoding, accuracy drops to 85.2% for Linear, 80.0% for SLERP, and 64.7% for TIES. Across both settings, most errors occur when the true operator is TIES, reflecting that TIES occupies a narrower regime and is easier to confuse with Linear or SLERP. Overall, these results support that similarity features capture the relationships that drive operator preference, and that a lightweight task encoding provides an additional, modest gain.

### F.2 Detailed Per-Task Results Across Merge Sizes

Tables 1–3 provide detailed per-task summaries for pairwise, three-way, and four-way merges of 7B checkpoints. For each task and merge method, we report the mean task performance, absolute differences from the expert and auxiliary baselines, and the corresponding relative changes. Highlighting the best fixed operator per task makes explicit how the strongest baseline varies across settings, while bolding *SIMMERGE* emphasizes its consistent advantage across tasks and merge sizes.

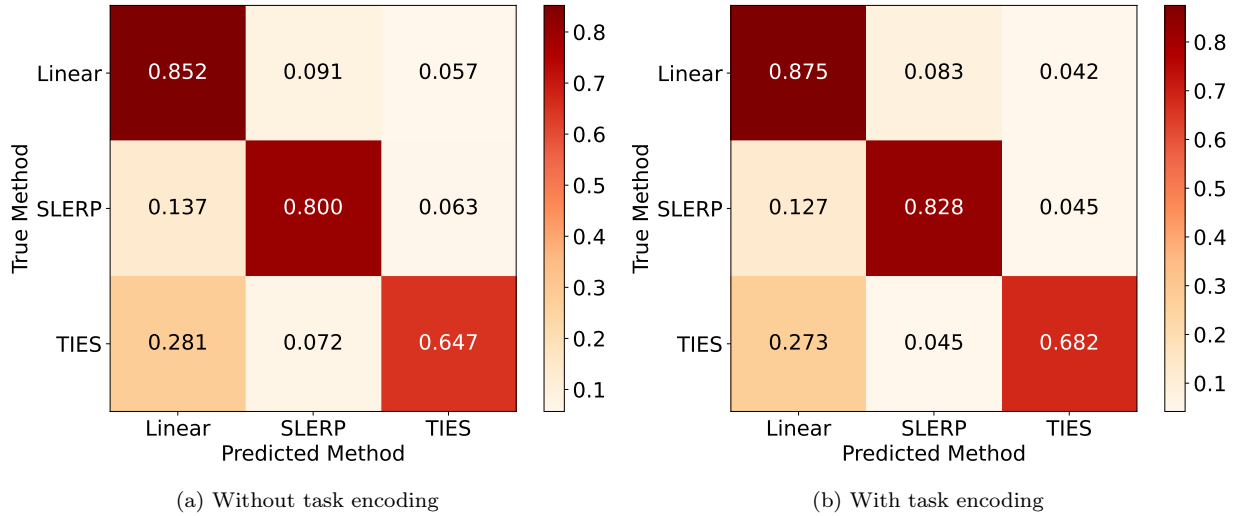


Figure 9: Confusion matrices of the offline selector on the held-out pairwise test set. Appending a task encoding improves per-class accuracy from 85.2% to 87.5% for Linear, from 80.0% to 82.8% for SLERP, and from 64.7% to 68.2% for TIES.

Task	Method	Mean	Diff.Exp	Diff.Aux	%Exp	%Aux
Code	Linear	0.60	-0.03	0.07	-4.70	12.31
	SLERP	0.59	-0.04	0.05	-7.07	9.52
	TIES	0.56	-0.07	0.02	-11.66	4.11
	<b>SIMMERGE</b>	<b>0.62</b>	<b>-0.02</b>	<b>0.08</b>	<b>-2.40</b>	<b>15.02</b>
Math	Linear	0.68	-0.07	0.11	-9.15	19.20
	SLERP	0.70	-0.05	0.13	-6.61	22.53
	<b>TIES</b>	<b>0.72</b>	<b>-0.03</b>	<b>0.15</b>	<b>-3.98</b>	<b>25.98</b>
	<b>SIMMERGE</b>	<b>0.74</b>	<b>-0.01</b>	<b>0.16</b>	<b>-1.90</b>	<b>28.80</b>
Multilingual	Linear	0.44	-0.16	0.09	-26.40	26.77
	SLERP	0.38	-0.22	0.03	-36.55	9.29
	TIES	0.32	-0.28	-0.03	-46.24	-7.40
	<b>SIMMERGE</b>	<b>0.46</b>	<b>-0.13</b>	<b>0.12</b>	<b>-22.27</b>	<b>33.89</b>
RAG	Linear	0.21	-0.20	-0.00	-49.46	-0.38
	<b>SLERP</b>	<b>0.25</b>	<b>-0.15</b>	<b>0.05</b>	<b>-37.65</b>	<b>22.88</b>
	TIES	0.22	-0.19	0.01	-46.09	6.26
	<b>SIMMERGE</b>	<b>0.28</b>	<b>-0.13</b>	<b>0.07</b>	<b>-32.11</b>	<b>33.81</b>

Table 1: Pairwise (2-way) merges: per-task performance summary. Mean is the task-level average score. Diff.Exp and Diff.Aux denote absolute differences from the expert and auxiliary baselines, %Exp and %Aux are the corresponding relative changes. The best fixed operator (among Linear, SLERP, and TIES) is highlighted in blue for each task, SIMMERGE is bold.

In the pairwise setting (Table 1), the best fixed operator differs substantially across tasks: Linear performs best on Code and Multilingual, TIES on Math, and SLERP on RAG. This variability confirms that no single merge operator dominates even in the simplest two-model regime. Across all tasks, SIMMERGE consistently achieves higher mean performance than the best fixed operator, simultaneously reducing degradation relative to the expert and improving more over the auxiliary baseline. These results establish that similarity features are predictive of operator choice and motivate learning instance-specific merge decisions.

For three-way merges (Table 2), overall performance decreases relative to the pairwise setting, reflecting

Task	Method	Mean	Diff.Exp	Diff.Aux	%Exp	%Aux
Code	Linear	0.60	-0.03	0.06	-5.39	11.77
	SLERP	0.57	-0.06	0.04	-9.18	7.29
	TIES	0.51	-0.12	-0.02	-18.68	-3.94
	<b>SIMMERGE</b>	<b>0.61</b>	<b>-0.02</b>	<b>0.08</b>	<b>-2.90</b>	<b>14.71</b>
Math	Linear	0.64	-0.09	0.04	-12.48	7.33
	SLERP	0.70	-0.03	0.11	-3.89	17.86
	<b>TIES</b>	<b>0.71</b>	<b>-0.02</b>	<b>0.11</b>	<b>-2.76</b>	<b>19.25</b>
	<b>SIMMERGE</b>	<b>0.73</b>	<b>-0.00</b>	<b>0.13</b>	<b>-0.02</b>	<b>22.61</b>
Multilingual	Linear	0.42	-0.15	0.08	-25.79	22.82
	SLERP	0.36	-0.21	0.02	-36.29	5.45
	TIES	0.34	-0.23	-0.00	-39.76	-0.30
	<b>SIMMERGE</b>	<b>0.44</b>	<b>-0.13</b>	<b>0.10</b>	<b>-22.20</b>	<b>28.77</b>
RAG	Linear	0.20	-0.20	-0.03	-49.76	-13.81
	<b>SLERP</b>	<b>0.22</b>	<b>-0.18</b>	<b>-0.01</b>	<b>-45.38</b>	<b>-6.30</b>
	TIES	0.21	-0.18	-0.02	-46.09	-7.52
	<b>SIMMERGE</b>	<b>0.24</b>	<b>-0.15</b>	<b>0.01</b>	<b>-38.88</b>	<b>4.85</b>

Table 2: Three-way ( $k=3$ ) merges: per-task performance summary using the same metrics as Table 1. The best fixed operator (among Linear, SLERP, and TIES) is highlighted in blue for each task; SIMMERGE is bold.

the increased difficulty of composing multiple models. Nevertheless, the same qualitative patterns persist: the identity of the strongest fixed operator remains task-dependent, and fixed baselines occasionally fail to improve over auxiliaries, particularly on RAG and Multilingual. In contrast, SIMMERGE consistently yields the highest mean performance across all tasks, incurring the smallest expert degradation while maintaining positive gains over auxiliary models in every domain.

Task	Method	Mean	Diff.Exp	Diff.Aux	%Exp	%Aux
Code	Linear	0.53	-0.08	0.01	-13.30	1.10
	SLERP	0.51	-0.10	-0.02	-16.89	-3.09
	<b>TIES</b>	<b>0.53</b>	<b>-0.08</b>	<b>0.01</b>	<b>-13.00</b>	<b>1.44</b>
	<b>SIMMERGE</b>	<b>0.59</b>	<b>-0.02</b>	<b>0.07</b>	<b>-3.36</b>	<b>12.68</b>
Math	Linear	0.69	-0.03	0.15	-4.70	27.01
	SLERP	0.68	-0.04	0.14	-5.54	25.67
	<b>TIES</b>	<b>0.71</b>	<b>-0.02</b>	<b>0.17</b>	<b>-2.09</b>	<b>31.59</b>
	<b>SIMMERGE</b>	<b>0.71</b>	<b>-0.02</b>	<b>0.17</b>	<b>-2.09</b>	<b>31.59</b>
Multilingual	Linear	0.38	-0.16	0.04	-29.95	11.54
	SLERP	0.33	-0.22	-0.01	-39.72	-4.01
	TIES	0.29	-0.26	-0.05	-47.19	-15.91
	<b>SIMMERGE</b>	<b>0.40</b>	<b>-0.14</b>	<b>0.06</b>	<b>-25.63</b>	<b>18.42</b>
RAG	Linear	0.18	-0.18	-0.03	-49.98	-14.11
	<b>SLERP</b>	<b>0.19</b>	<b>-0.16</b>	<b>-0.01</b>	<b>-45.07</b>	<b>-5.69</b>
	TIES	0.18	-0.17	-0.02	-48.22	-11.09
	<b>SIMMERGE</b>	<b>0.20</b>	<b>-0.15</b>	<b>-0.00</b>	<b>-42.01</b>	<b>-0.42</b>

Table 3: Four-way ( $k=4$ ) merges: per-task performance summary using the same metrics as Table 1. The best fixed operator (among Linear, SLERP, and TIES) is highlighted in blue for each task; SIMMERGE is bold.

Four-way merges (Table 3) further amplify the shortcomings of fixed operator choices. For several tasks, all fixed baselines incur large expert degradation and, in some cases, negative gains relative to auxiliaries, indicating harmful merges. Despite this increased complexity, SIMMERGE consistently remains

the top-performing method across tasks, often matching or exceeding the best fixed operator while substantially reducing expert degradation. These results demonstrate that similarity-driven operator selection becomes increasingly important as the number of merged models grows.

### F.3 Per-Task Trends Across Merge Sizes

Tables 1–3 report the exact per-task results for  $k \in \{2, 3, 4\}$ . Here we complement those tables with per-task trend plots that visualize how performance evolves with merge size under two reference points: (i) *expert-relative* change ( $\Delta_{\text{expert}}$ ), measuring preservation of task specialization, and (ii) *auxiliary-relative* change ( $\Delta_{\text{aux}}$ ), measuring retention of useful off-domain capability.

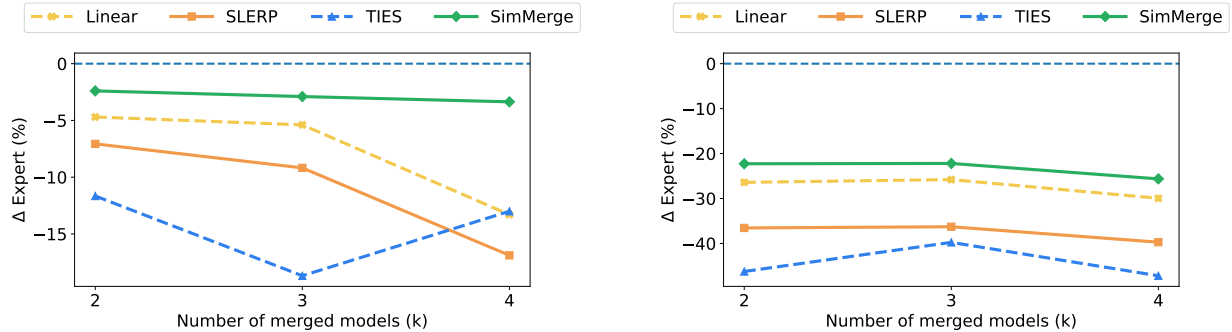


Figure 10: **Expert-relative trends.** Percentage change relative to the task expert ( $\Delta_{\text{expert}}$ ) as the number of merged models increases. Left: Code. Right: Multilingual. The effect of merge size can be non-monotonic (often a drop at  $k = 3$  followed by partial recovery at  $k = 4$ ), reflecting higher-order interactions between fine-tuned updates. Across both domains, SIMMERGE remains closest to the expert across merge sizes.

**Expert-relative trends (Code and Multilingual).** Figure 10 shows  $\Delta_{\text{expert}}$  as a function of  $k$  for Code and Multilingual. Across both domains, SIMMERGE remains closest to the expert at every merge size, forming the upper envelope among all methods. Notably, the effect of increasing  $k$  is not strictly monotonic: several fixed operators exhibit a pronounced degradation from  $k = 2$  to  $k = 3$  followed by partial recovery at  $k = 4$ . This non-monotonicity is consistent with multi-way composition dynamics, where the third model can introduce the first strong conflict between specialized updates, while adding a fourth model can partially cancel harmful directions under equal-weight merging. The Multilingual domain is particularly sensitive: fixed operators separate more dramatically as  $k$  increases, while SIMMERGE remains consistently closer to the expert.

**Auxiliary-relative trends (Math and RAG).** Figure 11 plots  $\Delta_{\text{aux}}$  for Math and RAG. As  $k$  grows, auxiliary gains can shrink or even become negative for fixed operators, indicating that naive multi-way merges can underperform the auxiliary baseline. This behavior is especially visible in RAG, where interference is strong and fixed operators often yield weak or negative auxiliary improvements. In contrast, SIMMERGE more reliably maintains positive (or near-zero) auxiliary gains across merge sizes, suggesting better retention of off-domain capability while still limiting expert degradation (Figure 10).

### F.4 Overall Gap Closed summary

Figure 2 reports domain-level averages of *Gap Closed*. To summarize overall performance with a single scalar, we take an unweighted macro-average across the four domain means on Code, Math, Multilingual, RAG.

To complement Table 4 and Figure 2, Figure 12 reports the corresponding average performance for the

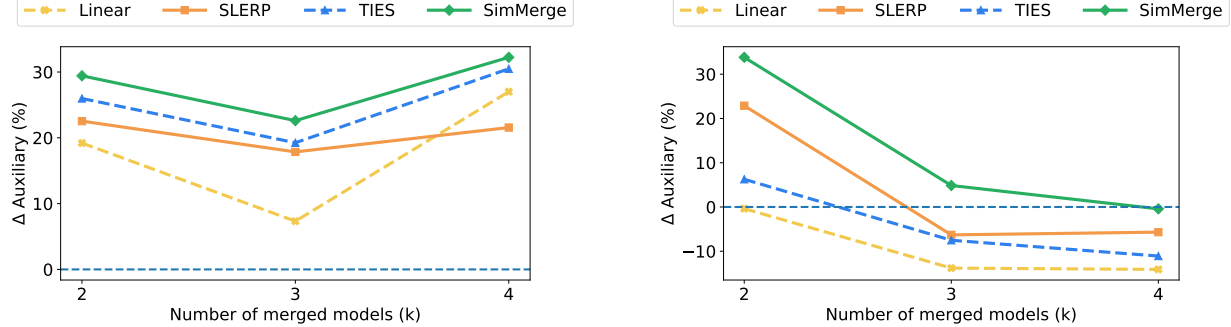


Figure 11: **Auxiliary-relative trends.** Percentage change relative to auxiliary baselines ( $\Delta_{\text{aux}}$ ) as the number of merged models increases. Left: Math. Right: RAG. Fixed operators can exhibit diminishing or negative auxiliary gains at larger  $k$ , particularly in RAG. SIMMERGE more consistently preserves improvements over auxiliaries across merge sizes, indicating more robust retention of off-domain capability under multi-way composition.

Method	Code	Math	Multilingual	RAG	Macro avg.
LINEAR	69.0	61.5	37.1	-0.4	<b>41.8</b>
SLERP	53.3	72.2	12.9	23.0	40.4
TIES	23.6	83.3	-10.2	6.4	25.8
SIMMERGE	84.2	94.3	46.9	34.8	<b>65.0</b>

Table 4: Domain-averaged GAPCLOSED from Figure 2 and macro-average across domains.

auxiliary, expert and merged models.

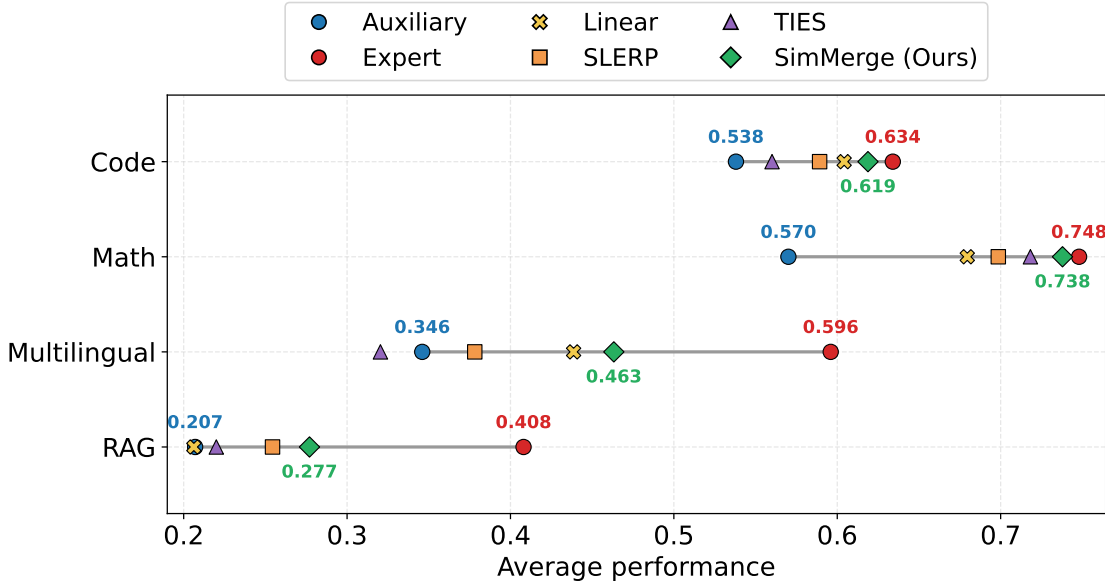


Figure 12: Absolute average performance per domain for auxiliary, expert, and merged models. This anchors the normalized metrics to the original task scales.

Figure 12 makes two points explicit on the original task scales. First, the expert-auxiliary gap differs substantially by domain. For instance, the expert improves over the auxiliary from 0.538 to 0.634 on Code, from 0.570 to 0.748 on Math, from 0.346 to 0.596 on Multilingual, and from 0.207 to 0.408 on RAG. Second, SIMMERGE consistently produces merged models that move toward the expert while improving over the auxiliary baseline across all four domains. In the pairwise setting, SIMMERGE

achieves the highest mean performance in every domain, reaching 0.62 on Code, 0.74 on Math, 0.46 on Multilingual, and 0.28 on RAG, outperforming the best fixed operator in each case. By contrast, the strongest fixed operator is domain-dependent: Linear on Code and Multilingual, TIES on Math, and SLERP on RAG, reinforcing that no single merge rule dominates across tasks. This absolute view also clarifies the trade-off: SIMMERGE improves off-domain performance while incurring smaller degradation relative to the expert than fixed baselines.

## F.5 111B task-level results for 3-way merges

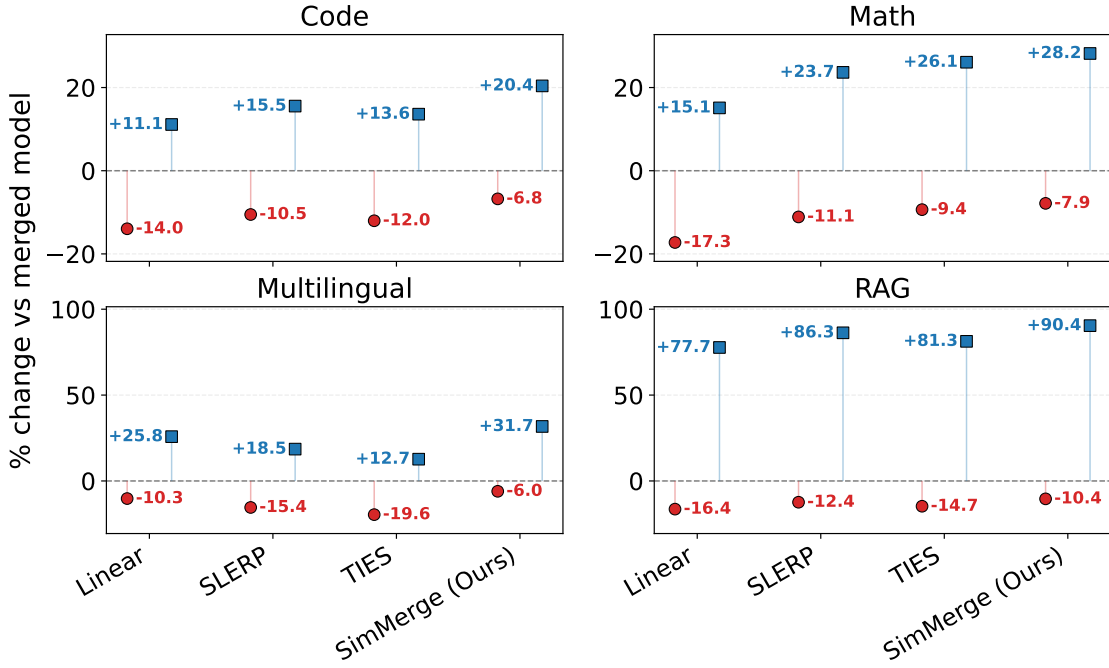


Figure 13: Per-task percentage change in performance for each merge method for 3-way merges at 111B. Blue markers show  $\Delta_{\text{aux}}$  (change vs. auxiliary; higher is better) and red markers show  $\Delta_{\text{expert}}$  (change vs. task expert; closer to 0 indicates less degradation), as defined in Section 3.4.

Figure 13 breaks down 3-way merging results at 111B by domain, reporting both auxiliary-relative gains  $\Delta_{\text{aux}}$  and expert-relative degradation  $\Delta_{\text{expert}}$  as defined in Section 3.4. Across all four domains, SIMMERGE achieves the strongest expert-auxiliary trade-off. It produces the smallest degradation relative to the expert in every domain, and it also delivers the largest gain over auxiliaries. For example, on Code it reduces expert-relative degradation to  $-6.8\%$  while improving over auxiliaries by  $+20.4\%$ . On RAG, it achieves a large auxiliary gain of  $+90.4\%$  while keeping expert degradation at  $-10.4\%$ .

Figure 14 reports the same comparison using GAPCLOSED, which normalizes performance so that 0% corresponds to the auxiliary baseline and 100% corresponds to the expert. SIMMERGE achieves the highest GAPCLOSED in every domain. The best fixed operator varies by domain, but SIMMERGE remains best overall, reaching 69.0 on Code, 76.6 on Math, 70.0 on Multilingual, and 80.3 on RAG.

## G Tail Effects and Similarity Correlations

We begin by examining how similarity signals correlate with merge operator performance. Figure 15 shows Pearson and Spearman correlations between similarity features and performance outcomes for LINEAR, SLERP and TIES across pairwise (PAIR), triple (TRIPLE), and quadruple (QUAD) merges.

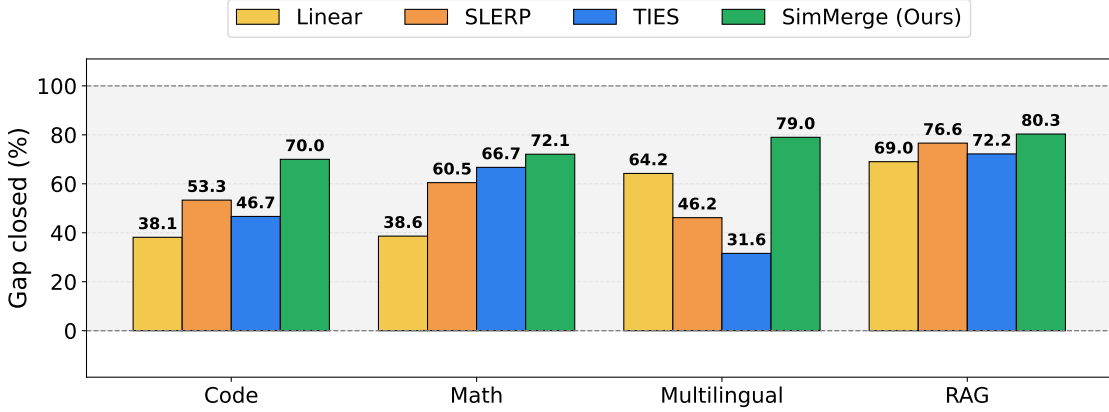


Figure 14: GAPCLOSED for 3-way merges at 111B across Code, Math, Multilingual, and RAG.

Several consistent patterns emerge. Across all merge settings, different similarity features are predictive of success for different operators, often with opposing signs. KL divergence is positively correlated with SLERP performance but negatively correlated with LINEAR, while weight cosine similarity exhibits the opposite pattern. Attention-based cosine similarity shows positive correlation with TIES, whereas weight  $\ell_2$  distance is most predictive of LINEAR’s success.

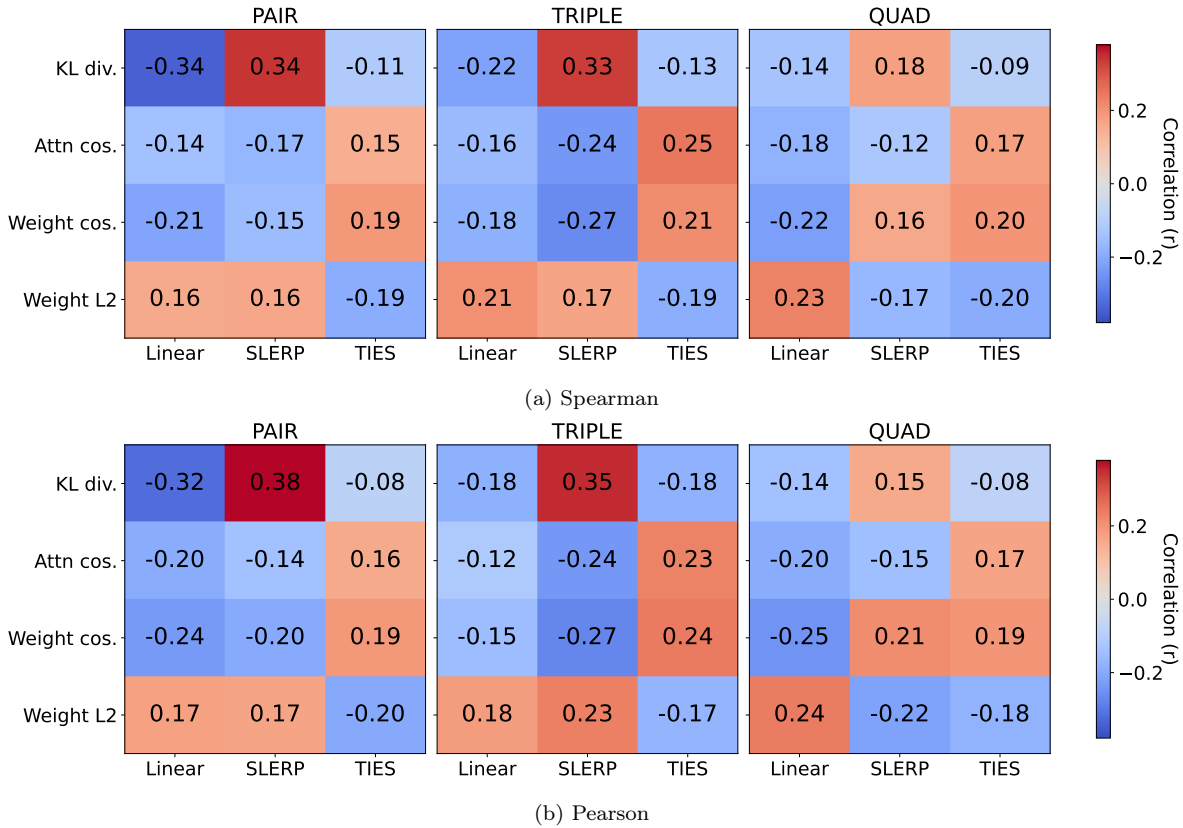


Figure 15: Correlation between similarity signals and merge performance for LINEAR, SLERP and TIES across pairwise, triple, and quadruple merges. Spearman and Pearson correlations exhibit consistent patterns, indicating robust, operator-specific similarity regimes.

The close agreement between Pearson and Spearman correlations indicates that these relationships are robust and largely monotonic rather than being driven by a small number of outliers. Importantly, no single similarity feature correlates positively with all operators, suggesting that merge quality is

inherently regime-dependent.

**Trends in percentile-bin.** The percentile-bin curves in Figure 16 visualize how each merge operator’s win probability ( $P(\text{win})$ ) varies as a function within-case percentiles. Overall, the directions of these trends are consistent with the winner-metric correlations shown in Figure 15.

Figure 16a shows that moving from low to high KL percentiles increases  $P(\text{win} = \text{SLERP})$  while decreasing  $P(\text{win} = \text{LINEAR})$  while TIES is weakly decreasing or near-flat.

In Fig. 16b,  $P(\text{win} = \text{TIES})$  increases monotonically with attention cosine similarity percentiles, while  $P(\text{win} = \text{LINEAR})$  decreases, SLERP tends to decrease, most clearly in the triple merge setting.

Figure 16c shows that higher weight-cosine percentiles favor TIES and disfavor LINEAR across merge settings. Notably, SLERP decreases with weight cosine in pairwise and triple merges but increases in QUAD, consistent with the corresponding sign flip observed in Figure 15. This pattern is consistent with spherical interpolation becoming more reliable when strong mutual parameter alignment is present in four-way merges.

Figure 16d shows that increasing weight  $\ell_2$  percentiles increase  $P(\text{win} = \text{LINEAR})$  and decrease  $P(\text{win} = \text{TIES})$  across merge settings. SLERP increases with  $\ell_2$  distance in PAIR and TRIPLE but decreases in QUAD, again mirroring the sign changes in Figure 15. This pattern is consistent with a geometric interpretation of the merge operators. Large weight  $\ell_2$  distance reflects substantial parameter magnitude mismatch between models. In such regimes, Linear interpolation, which does not rely on directional alignment, tends to be more robust, while TIES degrades due to increased trimming under magnitude differences. SLERP improves with increasing  $\ell_2$  distance in pairwise and triple merges but degrades in the quadruple setting, where averaging across multiple directions becomes less stable.

**Effects of merge size.** Comparing the panels within each subfigure in Figure 16, QUAD trends are often flatter, indicating weaker dependence on similarity percentiles. Additionally, SLERP exhibits two notable merge-size-dependent reversals: (i) a positive association with weight cosine similarity in QUAD (Figure 16c), and (ii) a negative association with weight  $\ell_2$  distance in QUAD (Figure 16d). These effects indicate that multi-model geometry introduces interactions beyond those captured by pairwise relationships.

**Tail effects and operator robustness.** While similarity-conditioned trends describe average behavior across similarity regimes, they do not capture how performance is distributed across individual merge instances. In particular, an operator may perform well on average while still failing catastrophically on a nontrivial fraction of cases. To characterize this behavior, we analyze *tail effects*, which quantify whether a method’s wins are concentrated in favorable regimes or whether it frequently appears among the worst-performing outcomes.

For each merge method, metric, and merge setting, we define the tail effect as

$$\Delta P(\text{win}) = P(\text{top 20\%}) - P(\text{bottom 20\%}) \quad (6)$$

where  $P(\text{top 20\%})$  denotes the probability that the method ranks in the top quintile of outcomes, and  $P(\text{bottom 20\%})$  denotes the probability of ranking in the bottom quintile. A large positive value indicates that a method consistently wins in favorable regimes while rarely failing badly, whereas values near zero or negative indicate brittle behavior with frequent severe failures.

Figure 17 visualizes tail effects across similarity metrics and merge settings. Fixed operators exhibit

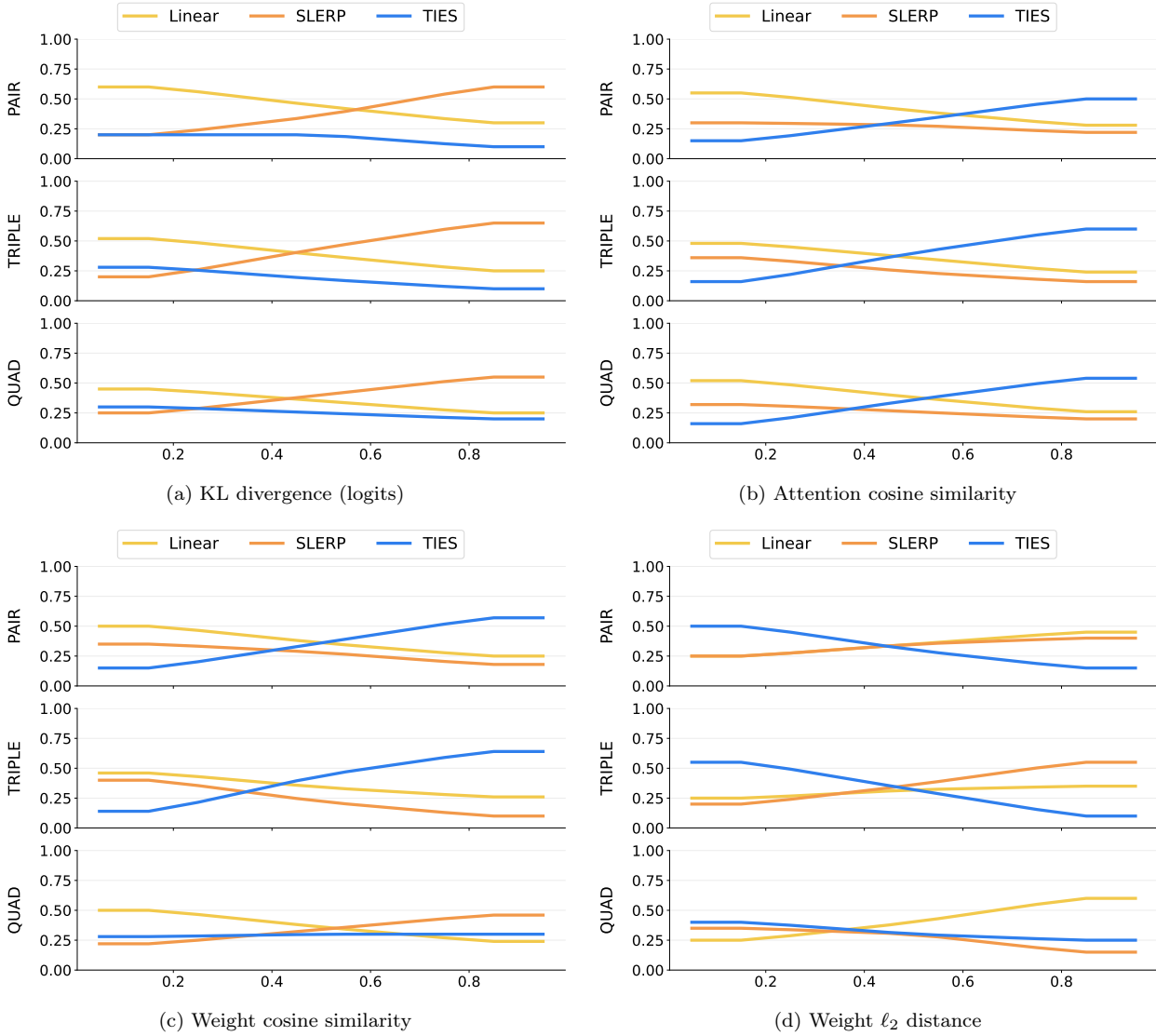


Figure 16: **Percentile-bin win trends.** For each case (PAIR/TRIPLE/QUAD), we map each probe metric to its empirical percentile and compute  $P(\text{win})$  for each merge operator within equal-mass percentile bins. This makes trends comparable across merges and across metrics with different raw scales.

strong and highly metric-dependent tail behavior. For example, LINEAR shows positive tail effects in regimes characterized by small weight distances, but negative or near-zero tail effects under KL divergence and attention-based similarity. Conversely, TIES concentrates wins when weight cosine or attention similarity is high, but frequently occupies the bottom tail outside these regimes. SLERP exhibits mixed behavior, with tail effects that change sign depending on both the similarity metric and the merge setting.

As merge complexity increases from pairwise to quad settings, tail effects generally become more pronounced. This indicates that applying a single operator uniformly across increasingly heterogeneous collections of models amplifies the risk of severe failures, even when average performance remains competitive. These tail failures explain why fixed operators can appear strong under aggregate metrics yet behave unreliably in practice.

Taken together, similarity-conditioned trends and tail effects show that merge operator effectiveness is inherently regime-dependent. Each operator succeeds only within specific similarity regimes and exhibits sharp failures outside them, leading to brittle behavior when a single rule is applied universally.

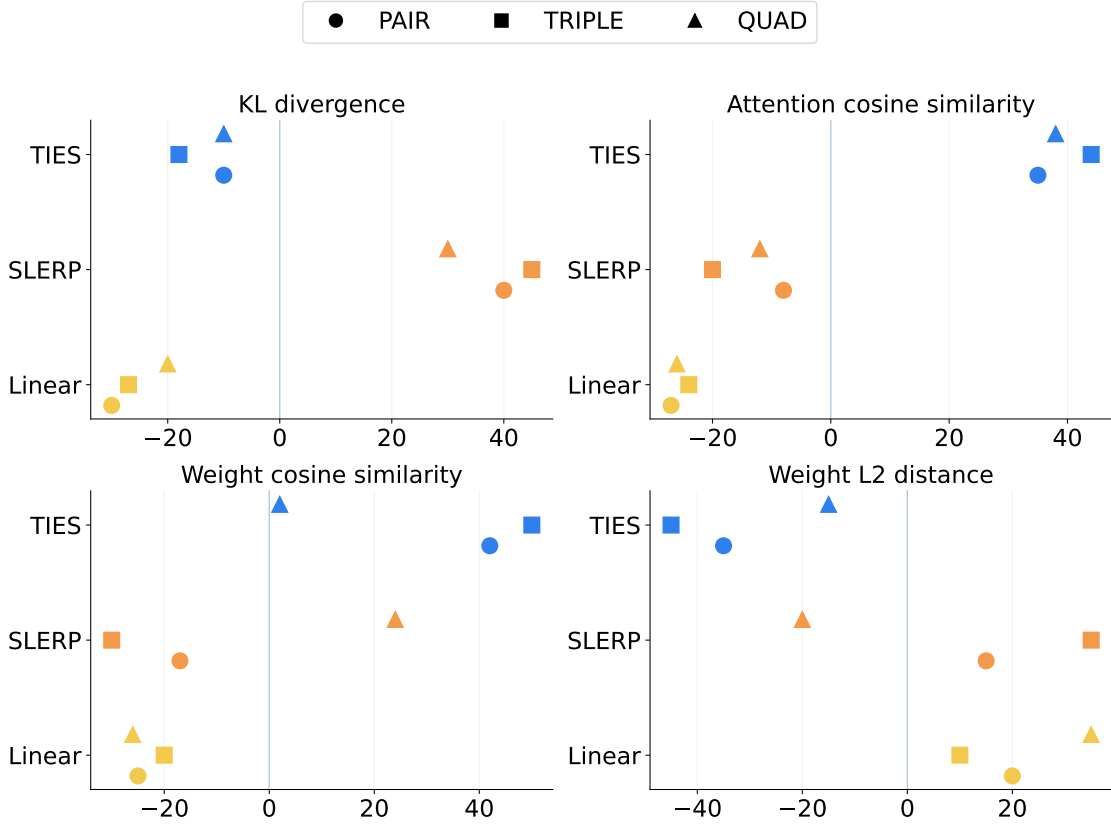


Figure 17: Tail effects of merge operators across similarity metrics and merge settings. Each point shows the tail-effect score (Eq. 6). Markers indicate pairwise, triple, and quad merges.

By identifying these regimes through similarity signals and selecting operators on a per-instance basis, SIMMERGE avoids unfavorable tails and achieves robust merging behavior across tasks and merge settings.